Feature Based Segmentation of Colour Textured Images using Markov Random Field Model

Thesis submitted in partial fulfillment
of the requirements for the degree of

Master of Technology
(Research)

by

Mridula J
(Roll No.: 608EE307)

under the supervision of

Dr. Dipti Patra

Department of Electrical Engineering
National Institute of Technology Rourkela
Rourkela–769 008, Odisha, India

March 2011

Department of Electrical Engineering
National Institute of Technology Rourkela
Rourkela–769 008, Odisha, India.

Certificate

This is to certify that the work in the thesis entitled *Feature Based Segmentation of Colour Textured Images using Markov Random Field Model* by *Mridula J* is a record of an original research work carried out by her under my supervision and guidance in partial fulfillment of the requirements for the award of the degree of Master of Technology (Research) during the session 2009–2011 under specialization in Electronic Systems and Communication, in the department of Electrical Engineering, National Institute of Technology Rourkela. Neither this thesis nor any part of it has been submitted for any degree or academic award elsewhere.

Dipti Patra
Associate Professor
EE department of NIT Rourkela

Place: NIT Rourkela
Date:

Acknowledgment

I have been very fortunate to have Dr. Dipti Patra, Associate Professor, Department of Electrical Engineering, National Institute of Technology, Rourkela as my thesis supervisor. She introduced me to the field of Image Processing and Computer Vision, educated me with the methods and principles of research and guided me patiently throughout this thesis work. She has been very liberal in supporting me all through to complete this study in time. She has been a perfect motivator, very cooperative and an inspiring guide to me to fulfill this academic pursuit. I am highly indebted and express my deep sense of gratitute to her. I am extremely thankful to herfor her incredible contribution in writing the manuscript.

I am extremely grateful to Prof. Sunil Kumar Sarangi, Director, N.I.T, Rourkela, and Prof. P. C. Panda for their encouragement and support in completion of this thesis. In particular, I would like to thank Prof. B. D. Subudhi, H.O.D, Electrical Engineering Dept., who kept an eye on the progress of my work and always was available when I needed his help and advises.

I humbly acknowledge the creative criticism and constructive suggestions of Prof. Susmita Das, Prof. B. Majhi and Prof. K. B. Mohanty, committee members, while scrutinizing my research work.

I am highly indebted to NIT Rourkela, for providing me all the facilities for my research work. I am extremely thankful to all the faculty members of the Department of Electrical Engineering, NIT, Rourkela for their encouragement and cooperation throughout this period. This work was made thoroughly enjoyable by the friendly and congenial atmosphere of Image Processing and Computer Vision Laboratory of Electrical Department. My heartfelt thanks to Kundan Kumar for the self initiative and the responsibility he took in every stage of my thesis writing. A special thanks to Subrajeet Mohapatra for helping and guiding me to learn Latex and complete my thesis early. I also thank Prajna, Venkateshwarulu and Sushanth for their support.

Many thanks to all the people whose friendship and companionship has given

a lot of encouragement during my research work. My profuse thanks to my close friends and neighbours Priya, Mitra Binda, Rajani, Madhusmitha, Radhika, Punyatoya and Mishra uncle for their unconditional support.

My deepest gratitude goes to my family for their unflagging love and support throughout my life. I shall always remain indebted to my parents for the continuous support they gave me and especially for taking care of my son Nenad during my absence which helped me to complete this thesis on time. I am also grateful and thankful to my mother-in-law and late father-in-law for their positive encouragement that they showered on me to complete this thesis. I also thank my sister Vinanthi for giving me moral support whenever I needed.

My little son, Nenad suffered a lot in my absence from home and I thank him profusely for his sense of understanding and unwavering faith in me.

Finally, I would end this note by placing my husband Mahesh at the bottom of my heart for the moral and emotional support he gave along with the tolerant effort he put to make this thesis complete, though equally busy with his own PhD thesis work. Moreover I thankfully appraise him that he accepted every difficult and challenging situation calmly from the begin to the end of this M Tech Research. I dedicate this work to all my family members.

Above all, I salute the divine powers, the Almighty for their abundant blessings for giving me strength and energy to complete this study successfully.

Mridula J

Abstract

The problem of image segmentation has been investigated with a focus on colored textured image segmentation. Texture is a substantial feature for the analysis of different types of images. Texture segmentation has an assortment of important applications ranging from vision guided autonomous robotics and remote sensing to medical diagnosis and retrieval in large image databases. But the main problem with the textured images is that they contain texture elements of various sizes and in some cases each of which can itself be textured. Thus the texture image segmentation is widely discerned as a difficult and thought-provoking problem. In this thesis an attempt has been made to devise methodologies for automated color textured image segmentation scheme.

This problem has been addressed in the literature, still many key open issues remain to be investigated. As an initial step in this direction, this thesis proposes two methods which address the problem of color texture image segmentation through feature extraction approach in partially supervised approach. The feature extraction approaches can be classified into feature based and model based techniques. In feature based technique features are assessed without any model in mind. But in case of model based approach an inherent mathematical model lets features to be measured by fitting the model to the texture. The inherent features of the texture are captured in a set of parameters in order to understand the properties generating the texture. Nevertheless, a clear distinction can not be made between the two approaches and hence a combination of approaches from different categories is frequently adopted.

In textured image segmentation, image model assumes a significant role and is developed by capturing salient spatial properties of an image. Markov random field (MRF) theory provides a convenient and consistent way to model context dependent entities. In this context a new scheme is proposed using Gaussian MRF model where the segmentation problem is formulated as a pixel labeling problem. The *a priori* class labels are modeled as Markov random field model and the num-

ber of classes is known *a priori* in partially supervised framework. The image label estimation problem is cast in Bayesian framework using *Maximum a Posteriori* (MAP) criterion and the MAP estimates of the image labels are obtained using iterated conditional modes (ICM) algorithm. Though the MRF model takes into account the local spatial interactions, it has a limitation in modeling natural scenes of distinct regions. Hence in our formulation, the first scheme takes into account within and between color plane interactions to incorporate spectral and contextual features. Genetic algorithm is employed for the initialization of ICM algorithm to obtain MAP estimates of image labels. The faster convergence property of the ICM algorithm and global convergence property of genetic algorithm are hybridized to obtain segmentation with better accuracy as well as faster convergence.

Another new scheme is developed by incorporating texture features computed using gray level co-occurrence matrix (GLCM) for color textured image segmentation. Besides image model, color model also plays a crucial role in color image segmentation. Hence, Ohta color space is used for better segmentation and the textural features of the image are computed using GLCM in Ohta color space. Thus obtained feature matrix is assumed to be the degraded version of the labeled image. The unknown class labels are modeled as MRF model. The model parameters are assumed to be known *a priori*. Segmentation is obtained by MAP estimation of image labels using ICM algorithm. In this proposed new scheme, incorporation of contextual feature using MRF model and textural feature using GLCM in Ohta color space obtains better segmented results for colored textured images. Both the proposed schemes are found to be outperforming the existing methods in terms of percentage of segmentation accuracy and time complexity.

Contents

List of Acronyms

MRF	Markov Random Field
GMRF	Gaussian Markov Random Field
GLCM	Gray Level Co-occurence Matrix
CON	Contrast
COR	Correlation
GA	Genetic Algorithm
ICM	Iterated Conditional Mode
ENT	Entropy
SA	Simulated Annealing
GD	Gibbs Distribution
GRF	Gibbs Random Field
HOM	Homogeniety
DIS	Dissimilarity
SD	Standard Deviation
ANG	Angular Momentum
MAP	Maximum a Posteriori
ML	Maximum Likelihood

Nomenclatures

W	Random field associated with the labels of the original image.
W_i	Random variable of i^{th} site of the original image.
X	Observed random field.
X_i	Random variable of the i^{th} site of the observed image.
x	Realization of X.
w	Realization of Y.
ϕ	Parameter associated with image model.
μ	Mean value of Gaussian distribution.
σ	Standard deviation of Gaussian distribution.
μ_p	Mean value of each class p with Gaussian distribution.
$P(.)$	Probability.
$P(.\|.)$	Conditional probability.
S	A rectangular image lattice.
(i, j)	A pixel of an image lattice.
$(M \times N)$	Size of the image lattice.
$\eta_{(i,j)}$	Neighbourhood of pixel (i, j).
$U(.)$	Energy function of Gibbs distribution.
Z	Partition function.
c	A clique.
C	Collection of all cliques.
$\text{dist}(A, B)$	Euclidian distance between A and B.
$V_c(.)$	Clique potential of MRF model.
x^*	True and unknown labeling configuration.
$\hat{x}$	Estimate for x^*.
$U_p(.)$	A posteriori energy function.
e_p	Spatial interaction of pixels in GMRF model.
v_{xy}	Expected value of $e_x e_y$.
$\sum$	Covariance matrix

μ_m	Mutation probability
μ_c	Crossover probability
W_{ij}	Posterior probability

List of Figures

List of Tables

Chapter 1

Introduction

"Vision - It reaches beyond the thing that is, into the conception of what can be. Imagination gives you the picture. Vision gives you the impulse to make the picture your own" quote by Robert Collier emphasizes the implication of the vision. Humans are fundamentally visual creatures. Vision allows humans perceive and realize the world surrounding them. The human visual system has the potentiality to acquire, integrate and interpret all the ample visual information around it [1,2]. Computer Vision aims to impart such challenging potentialities to a machine in order to interpret the visual information embedded in still images, graphics and video or moving images in our sensory world. It is astonishing when we realize just how much we are environed by images. Images allow us not only to perform complex tasks on a daily basis, but also to communicate, transmit information, represent and understand the world around us. Computer vision, image processing, image analysis, robot vision and machine vision are the terms that refer to some aspects of the process of computing with images. To accomplish this, computer vision techniques employ the results and methods of mathematics, computer science, electronics, pattern recognition, artificial intelligence and other scientific disciplines [2–4]. With the objective of easing the task of computer vision, two levels of processing are usually described as

- Low level image processing
- High level image understanding

In low level image processing, the input and output are both images. In a computer, an image is represented by a rectangular matrix with elements corresponding to the brightness at appropriate image locations. These images are the inputs and outputs for low level image processing. High level image understanding attempts to duplicate the human cognition and the power to arrive at decisions according to the information contained in the image. To begin with, high level vision takes some form of formal model of the world, compares the digital image encompassing the reality to the model and then switches to low level image processing to find the information needed to update the model. Low level computer vision techniques overlap almost with digital image processing. Image processing is not a one-step process. Thus we are able to distinguish between several steps which must be performed until we can extract the data of interest from the observed scene.

The following are the different steps that are seen in image processing

- Image Acquisition - This step involves capturing an image by a sensor and digitizing it.
- Image Enhancement - Includes suppression of noise and enhancing some object features which are pertinent to empathizing the image.
- Image Compression - Deals with the techniques for reducing the bandwidth needed for transmitting an image or the storage for saving an image.
- Image Segmentation - In this step the objects are separated from the image and from each other.
- Object Description - Also called feature selection, addresses the problem of extracting the attributes that contribute some quantitative information of interest.
- Recognition - Assigns labels to an object based on its descriptors.

Out of the above stated steps of digital image processing, this thesis deals with image segmentation. To be more precise, the thesis is dedicated on the

segmentation of the colour textured images stated in the Problem Definition.

1.1 Image Segmentation

Image segmentation can be defined as the process of partitioning an image into different regions that are homogeneous with respect to some image features. The goal of image segmentation is to detect and extract the regions which constitute an image. Identification of these regions is not involved in obstinate to the classification problem. Image segmentation can be thought of as the first look of a newly born baby at the world. That is to say, to gander without higher cognition on the objects that we see in the scene. In simple words, suppose we have an image with three regions, image segmentation simply says that, "there are three regions in the image" and the identification of the region is not a part of segmentation process. Each pixel in the image is labeled with the corresponding region number [5]. Using their visual sense, humans are able to partition their environment into distinguishable objects to help distinguish these objects, classify them, guide their movement and to perform almost every visual task. This includes analysis of colour, shape, motion and texture of objects, thus is a complex process. It may be a spontaneous natural activity for human visual system, but is not so easy to create an artificial algorithm that performs exactly as that of human visual system. Segmentation is the initiative step of any image analysis procedure and succeeding tasks such as feature extraction and objects recognition to a great extent rely on the quality of segmentation. In this way, the ultimate success or failure of the image analysis process depend exclusively on segmentation [6].

Many attributes such as gray level, colour, texture features, etc., can be taken into account during segmentation process. With the colour being a very powerful descriptor, colour images rendering incomparably more information than gray scale images, the colour image segmentation has earned significance in recent years. The other reasons being

- Availability of the state-of-the-art computers to process colour images.
- Reliability of the segmentation results with the colour images

- Managing of vast image databases, which are mainly constituted by colour images, as the Internet
- Irruption of 3G mobile phones, digital cameras and video sets.

However, simplifying assumptions made about the homogeneity of the colours in local image regions, in many image processing algorithms cannot be adopted in real images. This is due to the fact that real images exhibit deviation in intensities within a region which forms the texture. And this has necessiated the researchers to lead for colour textured image segmentation.

Texture can be defined as the repeating pattern of local spatial variations in pixel intensities of an image. It is important to note that tone and texture always form an integral part of an image. But one attribute can overshadow the other on occasions depending on the smoothness or coarseness of the surface of the objects. If the variation of the colour within a small area is comparatively small, then the tonal property will dominate. Contrarily, when there is a wide variation in the distribution of tone inside an area then the texture will become prevalent. Thus texture forms an innate attribute of all the objects. The small area which forms the fundamental unit of the texture is often called as a texel and a texture is categorized as smooth or coarse depending on the size of the texel. If texels are small and tonal deviation among texels is prominent, it results in a fine texture. While a coarse texture results from large sized texels consisting of several pixels. Even though many image segmentation techniques have been developed during the past years there is no universal method which can excellently perform the task for all type of images. In general the texture segmentation can be obtained through featured based, model based and hybrid methods. In our work we have considered the hybrid method in which the feature and model based approaches are combined. The method comprises of two stages viz., feature extraction and segmentation. Feature extraction process extracts the textural features which is then followed by segmentation. Segmentation is performed through model based approach which is categorized as (i) Supervised approach to segmentation and (ii) Unsupervised approach to segmentation

1.1.1 Supervised Image Segmentation

Supervised segmentation is an approach where the model parameters are assumed to be known *a priori* and are used for estimating the pixel lables in segmentation problem. The pixel labelling problem, using MRF model has been formulated using maximum *a posteriori* (MAP) criterion and Bayesian framework [7–9]. Segmentation of both noisy and textured images could be formulated in supervised frame work using MRF model. For Brain MR images, D. Patra have proposed Hybrid Tabu Search (HTS) algorithm to obtain the MAP estimates of the image labels and thus to accomplish supervised image segmentation [9].

1.1.2 Unsupervised Image Segmentation

In unsupervised framework, the number of class labels and model parameters are unknown and are to be estimated simultaneously. The unsupervised image segmentation is viewed as the incomplete data problem as the estimation of image labels depend upon the optimal set of parameters and vice versa. This type of problem is usually addressed using iterative schemes such as iterative conditional mode (ICM) algorithm which was initiated by Besag [8].

1.2 Application of Textured Image Segmentation

1. Remote Sensing application: As a first step in image analysis, segmentation of textured images plays a vital role in remote sensing applications which include

    - Classification of land cover classes
    - Tree species identification: Tree species identification is a very complex process. A given area of forest land is often occupied by a complex mixture of many tree species. The image characteristics like shape, size, pattern, shadow, tone and texture are used by interpreters for the process. The arrangement of tree crowns produces a pattern that is

distinct and give rise to different textures for different species. Thus segmenting the image according to these textures help in identification of the species.

- For crop type recognition in agricultural applications.
- To locate objects like detection of roads, to identify water bodies etc.

2. For robotic guidance

3. Medical applications: In medical imaging image segmentation is used to automatically extract the features from the image which are then used for variety of classification tasks such as

   - To differentiate normal tissue from abnormal one.
   - To locate tumors
   - Measure tissue volumes
   - Computer guided surgery
   - Diagnostic treatment planning
   - Study of anatomical structure

4. Document processing: In Document processing has applications ranging from postal address recognition to analysis and interpretation of maps. For example postal document processing include applications such as recognition of destination address and zip code information on envelopes. In these applications first step is the separation of image regions which contain useful information from background.

1.3 Literature Survey

Texture segmentation is a very significant operation in computer vision. As most natural surfaces show texture, a successful vision system must be capable to handle the textured world surrounding it. Specifically, the processing of colour textured

images has become an important issue due to its huge usage in computer vision applications. So it is a matter of significance to focus on both the features viz., colour and texture. Haralick [10, 11], Reed and du Buf [12] have made very good surveys on texture segmentation and feature extraction techniques and categorized texture segmentation techniques as feature based, model based and structural based approaches. The main difference between feature based and model based texture analysis is that texture features are measured without an ideal or model texture in mind in feature based techniques. But in model based approaches a mathematical model is assumed which allows features to be measured by fitting the model to the texture. However it is difficult to make a clear distinction as to which method is more suitable for texture segmentation and hence combinations of approaches are frequently adopted [13]. Kyong I. Chang *et. al.* [14] also reviewed unsupervised texture segmentation algorithms and conceptualized the control scheme of texture segmentation as two modular processes, (1) Feature computation and (2) Segmentation of homogeneous regions based on the feature values. The review of various methods of extracting textural features from images can also be found in [15] and [16] where in Mihran Tuceryan and A. K. Jain have presented the geometric, random field, fractal and signal processing models of texture in [15] and Stephen Haddad has investigated filter bank based methods and local descriptors in [16].

In feature extraction, properties of textures are derived from statistical measurements from the operation of filters or transformations. These include Gray Level Co-occurrence Matrices (GLCM), Laws texture energy (LAWS), Gabor filters, autocorrelation functions, second order spatial averages and two-dimensional filtering in the spatial and frequency domain etc. A.K. Jain *et. al.* have presented an unsupervised texture segmentation using Gabor filters and have proposed a systematic filter selection scheme [17]. This scheme is based on reconstruction of the input image from the filtered images and obtaining the texture features by subjecting each (selected) filtered image to a nonlinear transformation and computing a measure of "energy"in a window around each pixel. An unsupervised

square error clustering algorithm is then used to integrate the feature images and produce segmentation. Mihran Tuceryan has presented a texture segmentation algorithm based on the moments of an image [18]. In this algorithm, the moments within localized regions of the image around each pixel are computed followed by the estimation of a feature vector for each pixel based on these moments. Finally it segments these feature vectors (hence the texture regions) using a partitional clustering algorithm. Later, again, C. Palm and T. M. Lehmann proposed a method for classification of colour textures by using Gabor filters where in the Fourier domain is used for filter bank design and its implementation and Fourier transform is the main element of the Gabor transform [19]. Their study also confirms the colour to enhance the intensity texture features as well as composing an intensity independent pattern. M. Varma and A. Zisserman presented a texon based representation for texture classification suited to model the joint neighbourhood distribution for Markov random fields [20]. The representation is learnt from training images and then used to classify novel images into texture classes. From the studies it is found that the blurring in the filters means that the fine local details can be lost. Morten Rufus Blas *et. al.* have presented a fast integrated approach for online segmentation of colour and textured images for outdoor robot [21] by developing a compact colour and texture descriptor to describe local colour and texture variations in an image. Small neighbourhood vectors called textons that characterize scene textures are found out by clustering the neighbourhood vectors. Then histograms of textons are clustered over larger areas to find more coherent regions with the same mixture of textons. A texel-based approach to segment image parts occupied by distinct textures is proposed by Sinisa Todorovic and Narendra Ahuja [22]. Segmentation is done by capturing intrinsic and placement properties of distinct groups of texels. The scale or coarseness of texture is lower bounded by the size of its texels. To account for texel substructure, variable-bandwidth kernel in the mean shift has been derived and used a hierarchical.

Among the statistical approaches mention must be made on the use of gray level co-occurrence matrices (GLCM) to extract the textural features [23]. P. V.

Narasimha Rao *et. al.* have successfully implemented the GLCM approach to classify panchromatic satellite data using maximum likelihood classification [24]. Anne Puissant *et. al.* have utilized GLCM features for classification of high resolution imagery [25]. The methodology uses panchromatic band to extract the textural information and the three multispectral bands for spectral information. The output image generated by texture analysis is then used as an additional band to the multi-spectral bands and the four bands are then classed by a supervised classification by discriminant analysis. Very recently G. Christoulas *et. al.* have explored the textural characteristics of Medium Resolution Imaging Spectrometer (MERIS) data using GLCM for the classification of the image [26]. Despite the fact that GLCM was originally proposed in the context of texture classification, it has been applied to texture segmentation by many researchers [27–29].

In model based approach, segmentation of the textured images is done with the help of stochastic models like Markov random field (MRF) models. MRF theory is a branch of probability theory which provides a foundation for the derivation of the probability distribution of interacting features. It provides a systematic approach for depriving optimality criteria based on the *maximum a posteriori*(MAP) concept and tells how to model the *a priori* probability of contextual dependent patterns, such as textures and object features [30].

Panjwani and Healey have presented an unsupervised segmentation algorithm using Markov random field model for colour texture that captures spatial interaction within and between the bands of a colour image [31]. In the method the model parameters from image regions are estimated by maximum likelihood scheme and the final stage of the segmentation algorithm is a stepwise optimal merging process that at each iteration selects a merge that maximizes the conditional pseudolikelihood of the image. An important problem that has not been addressed in the scheme is the selection of neighbours during the design of colour random field models. Krishnamachari and Chellappa presented a multi resolution Gaussian Markov random field (MRF) model for texture segmentation in which coarser resolution sample fields are obtained by sub sampling the sample field at

fine resolution [32]. It was found that, although the Markov property is lost under such resolution transformation, coarse resolution non-Markov random fields can be effectively approximated by Markov fields. Again the concept of multi resolution Markov random field concept was adopted by Chang-Tsun Li for unsupervised texture segmentation. Chang-Tsun Li followed stochastic relaxation labeling to assign the class label with highest probability to the block site being visited and class information is propagated from low spatial resolution to high spatial resolution via appropriate modifications to the interaction energies defining the field [13]. Din-Chang Tseng and Chih-Ching Lai have demonstrated an evolutionary approach to unsupervised segmentation of Multispectral textured images using Markov random field model [33]. The powerful global exploration ability of genetic algorithm (GA) is utilized to improve MRF based segmentation approach for multi-spectral textured images. Yining Deng and B. S. Manjunath proposed a new method for unsupervised segmentation of colour textured images [34] which consisted of two independent steps (i) Colour Quantization and (ii) Spatial Segmentation. In the first step colours in the image are quantized to various classes which can be used to differentiate regions in the image. Then the image pixels are replaced by their corresponding colour class labels, which form a class-map of the image. The main aim of this work is on spatial segmentation, where a criterion for "good"segmentation using the class map is proposed. A region growing method is used to segment the image on the multiscale J-images. Many texture segmentation algorithms require the estimation of texture model parameters. The main aim of this paper is to segment images and video into homogeneous colour texture regions. A new approach called JSEG is proposed. This approach does not estimate a specific model for a textured region. But it tests for the homogeneity of a given colour texture pattern. Huawu Deng and David A. clause have presented a new implementation scheme by introducing variable weighting parameter to combine the region labeling component and the feature modeling component in a simple MRF based segmentation model [35]. Zoltan Kato *et. al.* proposed a new MRF image segmentation model which combines colour and texture features [36].

The proposed model relies on Bayesian estimation via combinatorial optimization (simulated annealing). The segmentation is obtained by classifying the pixels into different pixel classes represented by multi-variate Gaussian distributions. Perceptually uniform CIE-$L^*u^*v^*$ colour values are used as colour features and a set of Gabor filters as texture features. Ralf Reulke *et. al.* proposed a method for road detection in panchromatic images for traffic observation from airplane platforms [37]. As structure based approaches cannot be applied because of the limited image size the method utilizes texture based algorithms. Since MRF characteristics are independent of illumination of the observed area it is possible to minimize the influence of cast shadow - a common problem in natural scenes and hence it is shown that the method is suitable for the distinction of streets and surrounding areas. Recently Rahul Dey *et. al.* proposed a new Markov random field model known as constrained Markov random field model (CMRF) to model the unknown image labels and Ohta (I_1, I_2, I_3) model is used as colour model [38]. Discovering the inability of the MRF model to model the natural scenes, the proposed approach constrains the model based on the notion of Martingale to incorporate a stronger local dependence and hence to obtain segmentation for textured and natural scene images. The problem of colour image segmentation is addressed as a pixel labeling problem and the labels are estimated using Maximum *a posteriori* (MAP) estimation criterion. A hybrid algorithm is proposed to obtain the MAP estimate and the performance algorithm is found to be better than that of using Simulated Annealing (SA) algorithm. Very recently Halawani *et. al.* have also addressed the colour image segmentation problem using MRF model where in they have employed two colour models namely RGB and Ohta model [39]. A new MRF model called DMRF model is proposed to take care of intra colour plane and inter colour plane interactions. In RGB and Ohta model, the inter-plane correlation are decomposed and partial correlation has been introduced due to the DMRF model. A new hybrid algorithm in which SA algorithm is first run for some pre specified amounts of epochs and then ICM algorithm is run until the stopping criterion has been proposed. In order to protect edges an edge penalty function has been

introduced in the clique potential of the *a priori* model.

1.4 Motivation

Many image segmentation techniques exist for homogeneous colour regions. But natural scenes are rich in both colour and texture. Hence texture-segmentation is an essential initial step for texture-based image analysis and retrieval systems. But texture segmentation is a difficult problem, as the textured region can contain texture elements of various sizes, each of which can itself be textured. In addition to this, a unique solution of the texture segmentation problem is scarcely accomplishable because a generally accepted definition of texture is also missing. Due to this, texture analysis has been realized as one of the hardest areas in the field of computer vision and image processing. The principal consequences concerning the textured image analysis are to extract features followed by discrimination of the textured regions and to classify them. From the literature, it is seen that most texture segmentation algorithms require the estimation of texture model parameters, but are proved to be difficult. A region growing method based on image colour space quantization, named JSEG, is presented in [34] that provides good segmentation results on a variety of images and can obtain textured regions as well. But the segmentation in this approach is not based on texture features. Instead, they make use of other information such as colour and spatial arrangement to handle texture and thus it fails to segment real images accurately. Many feature based methods like filter banks, gray level co-occurrence matrices (GLCM), and model based approaches like Gaussian Markov random field (GMRF) models, multi resolution MRF models are also in use for texture segmentation. However the distinction cannot always be clearly made and a combination of approaches from different categories is frequently adopted. Thus the complications involved in texture segmentation have motivated the need for automatic segmentation techniques that are robust in application. The main objective of this thesis is to address the image segmentation schemes for colour textured images.

1.5 Problem Addressed

In this thesis, attempts are made to address the problem of colour textured image segmentation in partially supervised framework. The schemes have been proposed using feature based Markov random field(MRF) model. The research work of this thesis can be broadly categorized as:

1. Colour textured image segmentation using Gaussian Markov Random Field model (GMRF) and hybrid GA-ICM algorithm

2. Extraction of texture features using gray level co-occurrence matrix (GLCM) and utilizing the same for MRF model based colour textured image segmentation.

1.6 Summary of the Thesis

In this thesis, the problem of image segmentation in partially supervised framework is addressed. The focus is on colour textured and natural scene image segmentation. The observed image is assumed to be corrupted with white Gaussian noise. The problem is cast as a pixel labeling problem. The coloured textured images used in the thesis are taken from the web database i.e.,
"http://www.imageafter.com/", "http://www.cgtextures.com/"and
"http://www.eecs.berkeley.edu/Research/Projects/CS/vision/bsds/".

Taking inspirations from the work of D. Patra [9], Panjwani and Healey [31], P.V. Narasimha Rao *et. al.* [24], G. Christoulas *et. al.* [26] and Rahul Dey *et. al.* [38], feature based as well as model based approach is adopted for segmentation. The first method proposed studies colour textured image segmentation using compound Gaussian Markov Random Field (GMRF) model hybridized with genetic algorithm (GA). The Gaussian Markov random field (GMRF) model is a special case of Markov random field model(MRF) where the pixel value at location (i, j) statistically depends on the neighbouring pixels of the representing component together with the neighbouring pixels of the other components. Hence the model considers spatial interactions within each colour component and the inter-

actions between different components. The image label estimation is formulated in Bayesian framework using MAP criteria. Iterated conditional modes (ICM) algorithm is used for MAP estimation of image labels. As ICM algorithm heavily depends on initialization and has a probability of trapping into local minima, the global convergence property of GA is exploited to provide better initialization condition for ICM algorithm.

It is observed that the utilization of GA for the initialization does not guarantee proper initialization in each and every trial of the execution and hence fails to give accurate results in every trial. This problem could be circumvented with a new scheme which incorporates the features of gray level co-occurrence matrix (GLCM) in MRF model using Ohta colour space, to obtain texture segmentation with better accuracy. The method comprises of two stages, feature extraction and segmentation. In feature extraction, gray level co-occurrence matrix (GLCM) denoting the second order joint probability densities of each pixel gray level is computed. Then the statistical measures describing the texture are deduced from GLCM to obtain the texture feature matrix. The optimal texture feature matrix from a set of eight feature matrices is determined. Eight features matrices include angular momentum, contrast, correlation, dissimilarity, entropy, homogeneity, mean and standard deviation. Optimal feature matrix thus obtained is assumed to be the degraded version of the true labeled image and the segmentation of the feature matrix is done through MAP estimation using ICM algorithm.

1.7 Thesis Organization

The thesis is organized into the following chapters.

Chapter 1: Introduction

It starts with a brief introduction of image processing followed by the formal description of the problem of segmentation and significance of colouur and texture in image segmentation. It also includes literature survey, motivation and thesis contributions in brief.

Chapter 2: Background on Markov random field model, Gray Level Co-occurrence matrix and different colour models

This chapter focuses on background on Markov Random Field model and related models, Gray Level Co-occurrence Matrix, Genetic algorithm and the different colour models.

Chapter 3: Unsupervised segmentation of coloured textured images using Gaussian Markov random field model and Genetic algorithm

This Chapter studies colour texture image segmentation using compound Gaussian Markov Random Field (GMRF) hybridized with genetic algorithm. An attempt has been made to incorporate colour and contextual features by taking interactions within colour planes and between colour planes of RGB colour space using GMRF model [31]. Iterated conditional modes (ICM) algorithm is used for MAP estimation of image labels. GA is used for initializing the ICM algorithm.

Chapter 4: MRF model based image segmentation of colour textured images using GLCM

This Chapter proposes a new method which blends the features of gray level co-occurrence matrix (GLCM) and Markov random field model (MRF) to segment coloured textured images in Ohta colour space. Thus MRF model is used to incorporate contextual feature along with texture and colour feature. Ohta colour space is used for better segmentation. It is shown from the simulation that GLCM-GMRF-ICM scheme is found to be performing better than the scheme 1 proposed in chapter 3.

Chapter 5: Conclusion

This chapter presents concluding remarks on partially supervised segmentation schemes for colour textured images, with the scope for further work on the related problems.

1.8 Image Metrics

The quality of an image is examined by objective as well as subjective evaluation. The metrics used for comparison of performances of different segmentation schemes

are defined below.

Misclassification Error (MCE) is a measure of percentage of misclassified pixels changes their gray scale values in the segmented image. It measures the difference between two images. In other words, it measures the efficiency of the proposed schemes with the former existing schemes. Hence, the lower the value of MCE, better is the segmentation. The MCE can be calculated as

$$\% \text{ of MCE} = \frac{\text{Number of misclassified pixels in a region}}{\text{Total number of pixels in the region}} \times 100 \qquad (1.1)$$

Another image metric used for comparison of different methods is the execution time. Execution time is defined as the time taken for the simulation of an algorithm. The less time an algorithm takes for execution, the more efficient it is considered.

Subjective or Qualitative measure:

Subjective assessment is required to measure the image quality. Because of unavailability of quantitative performance measure in case of image segmentation, subjective or qualitative measure is another option for comparison. In a subjective assessment measures characteristics of human perception become paramount, and the image quality is correlated with the preference of an observer or the performance of an operator for some specific task. Hence, In usual case of image segmentation there is no quantitative performance evaluation measure because no ideal image can be used as reference. Any reasonable measure should be tuned to the human visual system. However perceptual quality evaluation is not a deterministic process. So, subjective evaluation is the way to prove the performance. Hence, human observer is the only way by which segmented image quality can be observed.

The processor used for simulation of the segmentation problem is **Intel Pentium D processor, 2.80 GHz, 1 GB RAM, Fedora-10 version in Linux operating system using C language**.

Chapter 2

Background on Markov Random Field Model, Gray Level Co-occurrence Matrix and Different Colour Models

2.1 Introduction

Image Segmentation techniques using spatial interaction models like Markov Random Field (MRF) and Gibbs Random Field (GRF) to model the image have been very popular recently. The use of contextual information is indispensable in low level as well as high level Image Processing. Markov Random Field theory provides a convenient and consistent way of modeling the entities with contextual constraints. This is achieved through characterizing mutual relationship among such entities such as pixels of an image and other spatially correlated features using MRF probabilities. MRF forms a probabilistic model for a set of variables that interact on a lattice structure. This started with the influential work of Geman and Geman [7] who linked via statistical mechanics between mechanical systems and probability theory. The distribution for a single variable at a particular site is conditioned on the configuration of a predefined neighbourhood surrounding that site. This chapter gathers together the background information of Markov Random Field.

2.2 Markov Random Field

Let us consider a collection of random variables $X_{i,j}$, that is a random field defined over a finite discrete rectangular lattice of size $(M \times N)$. The lattice S is defined as $S = \{(i,j)\colon 1 \leq i \leq M, 1 \leq j \leq N\}$ where site (i,j) corresponds to each pixel of the discrete image lattice structure. A neighbourhood system η on this rectangular lattice can be defined as follows,

Definition 1 A collection of subsets of S described as $\eta = \{\eta_{i,j}\colon (i,j) \in S, \eta_{i,j} \subset S\}$ is a neighbourhood system on S if and only if $\eta_{i,j}$, the neighbourhood of pixel (i,j) is such that

1. a site is not neighbouring to itself: $(i,j) \notin \eta_{ij}$
2. the neighbouring relationship is mutual : If $(k,l) \in \eta_{ij}$, then $(i,j) \in \eta_{kl}$ for any $(i,j) \in S$

The neighbour set of η_{ij} is defined as the set of nearby sites within a radius r such that $\eta_{ij} = \{(k,l) \in S \mid \{dist((i,j),(k,l))\}^2 \leq r, (i,j) \neq (k,l)\}$, where $dist(A,B)$ denotes the Euclidean distance between A and B, r takes an integer value. A hierarchically ordered sequence of neighbourhood systems is shown in Figure 2.1 where η^1, η^2, η^3 ... are the "first-order", "second-order", "third-order"... neighbourhood systems respectively and are denoted by numbers $1, 2, 3...$ as shown in Figure 2.1 Due to the finite lattice used, the neighbourhood of pixels on the boundaries are necessarily smaller unless a toroidal (periodic) lattice structure is assumed. A nearest neighbourhood dependence of pixels on an image lattice is obtained by going beyond the assumption of statistical independence. the neighbourhood systems that can be defined over S are neither limited to the hierarchically ordered sequence of neighbourhood systems, nor they have to be isotropic or homogeneous.

Definition 2 Let η be a neighbourhood system defined over a lattice S. A random field $X = \{X_{i,j}\}$ defined over lattice S is a Markov Random Field (MRF) with respect to the neighbourhood system η if and only if

1. All of its realizations have non zero probabilities

   $P(X = x)>0$ for all x (property of positivity)

2. Its conditional distribution satisfies the following property

   $P\{X_{ij} = x_{ij} \mid X_{kl} = x_{kl}, (k,l) \in S, (k,l) \neq (i,j)\}$

   $= P\{X_{ij} = x_{ij} \mid X_{kl} = x_{kl}, (k,l) \in \eta_{ij}\}$ for all $(i,j) \in S$ (property of Markovianity)

where x_{ij} is the configuration corresponding to the random variables X_{ij} and so on. When the positivity condition is satisfied, the joint probability $P(X)$ of any random field is uniquely determined by its local conditional probabilities [40]

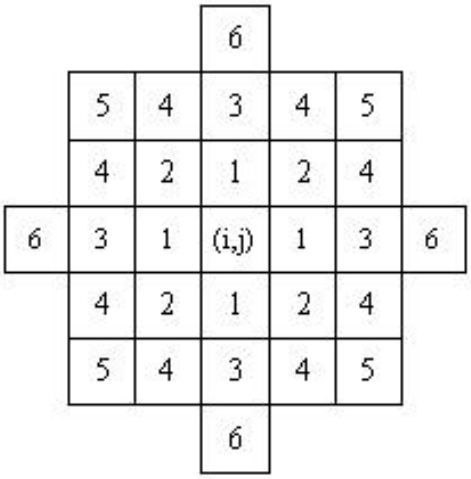

Figure 2.1: Hierarchically arranged neighbourhood system of Markov random Field

The Markovianity depicts the local characteristics of X which is characterized by the conditional distributions. The *Definition 2* says that the image value at a pixel does not depend on the image data outside the neighbourhood, when the image data on its neighbourhood are given. Hence, the most attractive feature of MRF is that *"images tend to have a degree of cohesiveness*: *pixels located near to each other tend to have the same or similar colours "* [7]. It doesn't constitute a theoretical restriction either, because all random field satisfy *Definition 2*, with respect to a large enough neighbourhood system, e.g. $\eta = S$ for all $\eta \in S$. On the other hand, MRF models, even with respect to small neighbourhood systems such as η^2 prove to be very flexible and powerful. Let us define the clique associated

with (S, η), a lattice neighbourhood system pair:

Definition 3 A clique of the pair (S, η) denoted by c is a subset of S such that

1. c consists of a single pixel, or
2. for $(i, j) \neq (k, l)$, $(i, j) \in c$ and $(k, l) \in c$ implies that $(i, j) \in \eta_{k,l}$

The collection of all cliques of (S, η) is defined by $C(S, \eta)$. The clique types associated with first-order and second-order neighbourhood systems.

2.3 Gibbs Random Field

Gibbs Distribution (GD) or equivalently the Gibbs Random Field (GRF) can be defined as follows,

Definition 4 Let η be a neighbourhood system defined over a finite lattice S. A random field X is said to be a Gibbs Random Field (GRF) of lattice S with respect to a neighbourhood system η if and only if its configuration obey a Gibbs distribution which has the following form

$$P(X = x) = \frac{1}{Z} e^{-\frac{1}{T}U(x)} \tag{2.1}$$

where,

$$Z = \sum_{x} e^{-\frac{1}{T}U(x)} \tag{2.2}$$

is the partition function. Z is simply a normalizing constant so that the sum of the probabilities of all realizations, x becomes one. T is a constant analogous to temperature which shall be assumed to be 1 unless otherwise stated and $U(x)$ is the energy function or Hamiltonian of a Gibbs distribution, which can be expressed as follows

$$U(x) = \sum_{c \in C} V_c(x) \tag{2.3}$$

Hence, energy is sum of clique potentials $V_c(x)$ over all possible cliques C. $V_c(x)$ are a set of potential functions depending on the values of x at the sites in the clique c. Thus, the key functions in determining the properties of the distribution are the potential functions $V_c(x)$. $P(x)$ measures the probability of the occurrence

of a particular configuration x. The more probable is a particular configuration, has lesser energy. This is so because the energy is computed as a measure of the distance between the model and the raw image data. The potential functions are chosen to reflect the desired properties of the image so that the more likely images have a lower energy and are thus more probable. The temperature T controls the sharpness of the distribution. When the temperature is high, all configurations tend to be equally distributed and when it gradually decreases to zero , global energy minima is achieved. Gibbs energy formalism has the added advantage that if the likelihood term is given by an exponential, and the prior is obtained through a MRF model, The posterior probability continues to be a gibbsian. This makes the MAP estimation problem equivalent to an energy minimization.

2.4 Markov-Gibbs Equivalence

An MRF is defined in terms of local properties (the classification label assigned to a pixel is affected only by its neighbours), whereas a GRF is characterized by its global property(the Gibbs distribution). The popular Hammersley-Clifford's stats that "*given the neighbourhood structure η of the model, for any set of sites within the lattice S, their associated contribution to the Gibbs energy function should be non zero, if and only if the sites form a clique; a random field's having the Markov property is equivalent to its having a Gibbs distribution*". This theorem establishes the equivalence of these two types of properties and provides a very general basis for the specification of MRF joint distribution function. Many have been used through out the literature [30]. The difficulties inherit in the MRF formulation are eliminated by use of this equivalence which are as follows:

1. Readily available joint distribution of random field
2. obtaining local characteristics regardless of inconsistency
3. Characterizing the Gibbs Distribution model with few parameters

By the use of MRF-GRF equivalence, MRF theory provides a mathematical foundation for solving the problem of making a global inference using local infor-

mation. It follows from the above equivalence that the local characteristics of the MRF are readily obtained from the joint distribution in 2.1 as

$$\begin{aligned} P(X_{i,j} = x_{i,j} \mid X_{k,l} = x_{k,l} \in S, (k,l) \neq (i,j)) \\ = P(X_{i,j} = x_{i,j} \mid X_{k,l} = x_{k,l}, (k,l) \in \eta_{i,j}) \\ = \frac{e^{-\sum c \in CV_c(x)}}{\sum x_{i,j} \in S e^{-\sum c \in CV_c(x)}} \end{aligned} \tag{2.4}$$

2.5 Line Process

In MRF models, smoothness is a generic contextual constraint which makes the assumption that the physical properties in a neighbourhood space exhibit some spatial coherence and homogeneity of image lattice [7]. However improper imposition of it can lead to undesirable, over-smoothed solutions. It is essential to take care of discontinuities when using smoothness prior. To avoid the problem of over-smoothing Geman and Geman [7] proposed combing the underlying MRF(intensity process) with an additional "line process".

The line process is neither a data nor the target of estimation. Rather, it is an adjunct process which is coupled to the intensity process in such a manner that the joint probability distribution of intensity function is locally smooth with line process for discontinuities. The prior on the line process is often chosen to accentuate continuous lines and to reject spurious edge elements. Such a model has the desirable property of promoting structure within the image without causing over smoothing. A couple of MRFs are defined on the image lattice, one is for intensity or label field, other is the dual lattice for the edge field or "line field". A line process comprises a lattice S' of random variable $f \in F$, whose sites $i' \in S'$ corresponded with vertical and horizontal boundaries between adjacent pixels of the image lattice. It takes the value from $\{0, 1\}$ which signifies the absence or occurrence of edges. $f_{i'} = 1$ of the line process variable indicates that a discontinuity is detected between neighbouring pixels j and i, i.e. $V_{(i,j)}(x_i, x_j)$ is considered as 0 or the bond between two pixels is 0; $f_{i'} = 0$ indicates continuity between above two pixels and $V_{(i,j)}(x_i, x_j)$ is taken same as before.

Another neighbourhood N is defined over the dual lattice S' for line sites. each pixel has four line site neighbours. Image lattice can be represented as S $\cup$ S$'$. The Eqn.(2.1) can be represented with the incorporation of line field as

$$P(X = x, F = f) = \frac{1}{Z} e^{-\frac{1}{T}U(x,f)} \tag{2.5}$$

The resulting MAP estimation can therefore be defined using a Gibbs posterior distribution whose prior energy function is

$$U(x, f) = U(x \mid f) + U(f) \tag{2.6}$$

Assignment of line field is preferred as it results in smaller energy and better estimation. The fundamental concepts underlying a line process were further addressed by Geman and Reynolds [41]. They suggested the proper potential function for cost measurement, giving a prior on the line process, to provide the ability to model transitions in gray level.

2.6 Gibbs Sampler

To implement the Relaxation algorithm, Geman and Geman [7] developed the Gibbs Sampler to explore the energy surface. The interpretation of the Theorems derived by them are as follows,

- The interpretation of the **Theorem A** is *"At constant temperature, if each site of an image lattice is visited infinite times, as time to infinity, the configuration X will be a sample from the Gibbs distribution and this distribution is independent of the initial configuration".*

- The interpretation of the **Theorem B** is *"To reach equilibrium state with lowest energy, the temperature is forced to decrease slowly. As time to infinity, X will be a sample from the Gibbs distribution at temperature absolute zero degree or the Gibbs distribution with minimum energy".*

The Gibbs sampler works by updating each random variable individually, but conditional on the states of the surrounding sites. The sequential implementation

corresponding to a raster scan is used for Gibbs sampler. The state of image evolves by discrete changes.So for convenience time is discretized, say $t = 1, 2, 3...$ At a given time, each site $x_{i,j}$ is represented by a random variable $X_{i,j}(t)$ with values in $G = 0, 1, 2, ..., n-1$. Hence the total configuration of the image is $X(t) = \{x_{i,j}(t)\}$; $i, j \in$ S. The starting configuration $X(0)$ is arbitrary and at any time t, the total configuration $X(t)$ evolves due to state change of individual site. At any instant of time only one state undergoes change. So the state at any two consecutive instant of time t and t-1 can differ by at most one coordinate. If n1,n2,...be the sequence in which the sites are visited for replacement; thus $n_t \in$ S and $X_{i,j}(t) = X_{i,j}(t-1)$, $i \neq n_t$. For replacement at each site a sample is drawn from its local characteristics. In other words, a state $x \in Gn_t$ is chosen from the conditional distribution of X_{nt}. Given the observed states of the neighbouring sites. All other sites remaining unchanged, the change in total energy is the changes due to change at site n_t with respect to its neighbourhood. Let $U(t-1)$ is the old energy and $U(t)$ be the new one. If $U(t)$ is found to be less than $U(t-1)$, then the change is accepted; otherwise the old energy $U(t-1)$ is retained. Wen all the sites of the image are visited once, one iteration is said to be completed.

2.7 Gray Level Co-occurrence Matrix (GLCM)

Texture is an imperative feature used in visual interpretation and segmentation of images. One of the delineating characters of the texture is the spatial distribution of gray values. The widely used approaches to depict the distribution are the statistical, structural and spectral approaches and the approach based on the employment of statistical features is one of the early and simple methods. The statistical approaches employ the first, second, third and higher order texture measures for texture calculation. First order texture measures are statistics calculated from the original image measures and do not look at pixel neighbour relationships. They utilize statistical moments of the histogram of an image. The moments include first order moment, mean, second order moment, variance or higher order moments like skewness, kurtosis etc. But this technique suffers from

an impediment that it does not contain any information concerning the relative position of pixels with respect to each other. The best way to recover from this is the application of second order statistical measures. In recent years, there is a tendency in signal processing to replace the methods based on second order statistics by higher order statistics. But it has also been found that higher order statistics have been very useful in problems where non-Gaussianity, nonminimum phase, colored noise or nonlinearity is important. In our thesis as we have taken into account the Gaussian noise and Markov Random field model, we have focused on second order statistics which is more suitable.

A long-familiar statistical tool for extracting second-order texture information is the gray level co-occurrence matrix. Given an N x N image composed of pixels each with an intensity in the range $\{0, 1, .., G-1\}$, the GLCM is an exemplification of how frequently different combinations of gray levels concur in an image. A GLCM denote the second order conditional joint probability densities of each of the pixels, which is the probability of occurrence of grey level i and grey level j within a given distance d and along the direction θ. Thus there may be multiple numbers of cooccurrence matrices depending on various values of d and 'θ'. GLCM involves the relation between a pair of pixels at a time. Let the two pixels be called as the reference and the neighbour pixel. The neighbour pixel is chosen from one of the four directions namely horizontal, vertical, left diagonal and right diagonal. Each direction denotes the angles 0^o, 90^o, 135^o and 45^o respectively. This is shown in figure 2.2. Thus GLCM is established by calculating how often a pixel with the gray level i occurs in a specific spatial relationship to a pixel with the value j.

2.7.1 Genetic Algorithms

Genetic algorithms (GAs) are numerical optimization algorithms inspired by both natural selection and natural genetics. They belong to a class of search techniques that mimic the principles of natural selection to develop solutions of large optimization problems.

Genetic algorithms work with the following primal elements,

A. **Chromosomes:**:

Strings that encode candidate solutions are called chromosomes. These are raw genetic information that GA deals with.

B. **Gene:**

A gene is a subdivision of the chromosome which represent individual component of the chromosome.

C. **Population:**

Collection of chromosomes is known as population.

D. **An objective or fitness function:**

Fitness function is the one that represents the degree of goodness of the string and is associated with each string. This fitness function is used to guide the stochastic selection of the chromosomes which are then utilized to generate new candidate solutions. The choice of fitness function bears a very authoritative role [42, 43].

The operations that are identified in GA are Fitness compution using objective function, selection, crossover and mutation and these are dicussed in detail in Chapter 3

2.7.2 Creation of Gray Level Co-occurrence Matrix

GLCM is established by calculating how often a pixel with the gray level i occurs in a specific spatial relationship to a pixel with the value j. The spatial relationship refers to the distance d and angle θ. For example, the value contained in cell (2, 4) represents the number of times that gray levels 2 and 4 occur with a specific direction and distance. Fig 2.3 illustrates the general form of the GLCM. Figures 2.4 through 2.7 demonstrate the results for four directions 0° (horizontal), 90° (vertical), 45° (right diagonal) and 135° (left diagonal) respectively, with distance d = 1. Then the obtained values are normalized to the range [0, 1] to avoid scaling effects. The normalized values are obtained for each cell in the matrix by

computing the total number of nearest neighbour pairs and the procedure for the computation is as follows,

- For the horizontal direction, considering d = 1, there will be 2 × (number of columns - 1) pairs in each row. Accordingly, the total number of nearest neighbour pairs can be found by the generalized expression
  2 × (number of columns - 1) × (number of rows) .

- For the vertical direction, with d = 1, there will be 2 × (number of rows - 1) pairs

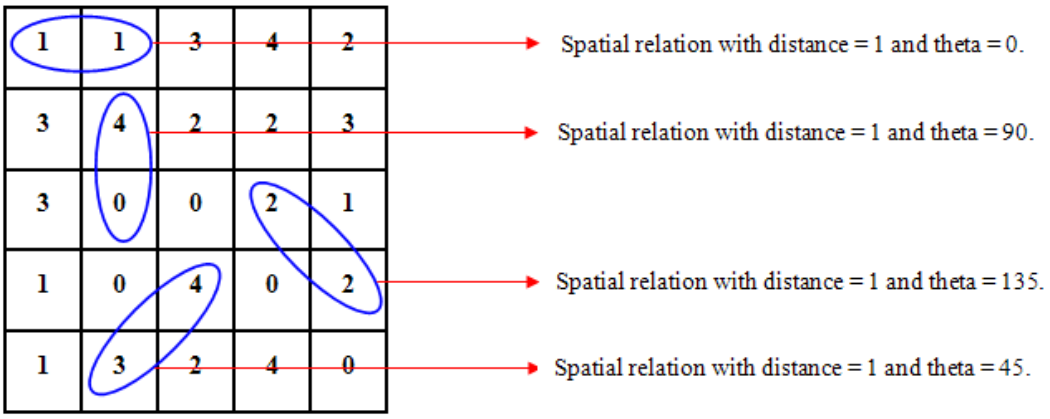

Figure 2.2: spatial relationship of a pixel with gray level i to a pixel with gray level j

in each column. So the total number of nearest neighbour pairs will be equal to
2 × (number of rows - 1) × (number of columns)

- For the left diagonal direction, with d = 1, 2 × (number of columns - 1) pairs will be present for each row except the last. This constitutes for the total number of pairs equal to
  2 × (number of columns - 1) × (number of rows - 1).

- Similarly, by symmetry, the number of nearest neighbour pairs for the right diagonal direction again with distance d =1, is same as that of the left diagonal.

After having the total number of pairs for each matrix, each matrix is normalized by

$$Normalized\ value = \frac{Value\ at\ each\ location}{Total\ number\ of\ pairs}$$

Gray Level →	0	1	2	3	4
0	(0,0)	(0,1)	(0,2)	(0,3)	(0,4)
1	(1,0)	(1,1)	(1,2)	(1,3)	(1,4)
2	(2,0)	(2,1)	(2,2)	(2,3)	(2,4)
3	(3,0)	(3,1)	(3,2)	(3,3)	(3,4)
4	(4,0)	(4,1)	(4,2)	(4,3)	(4,4)

Gray Level ↓

Figure 2.3: General Form of GLCM with gray values [0-4]

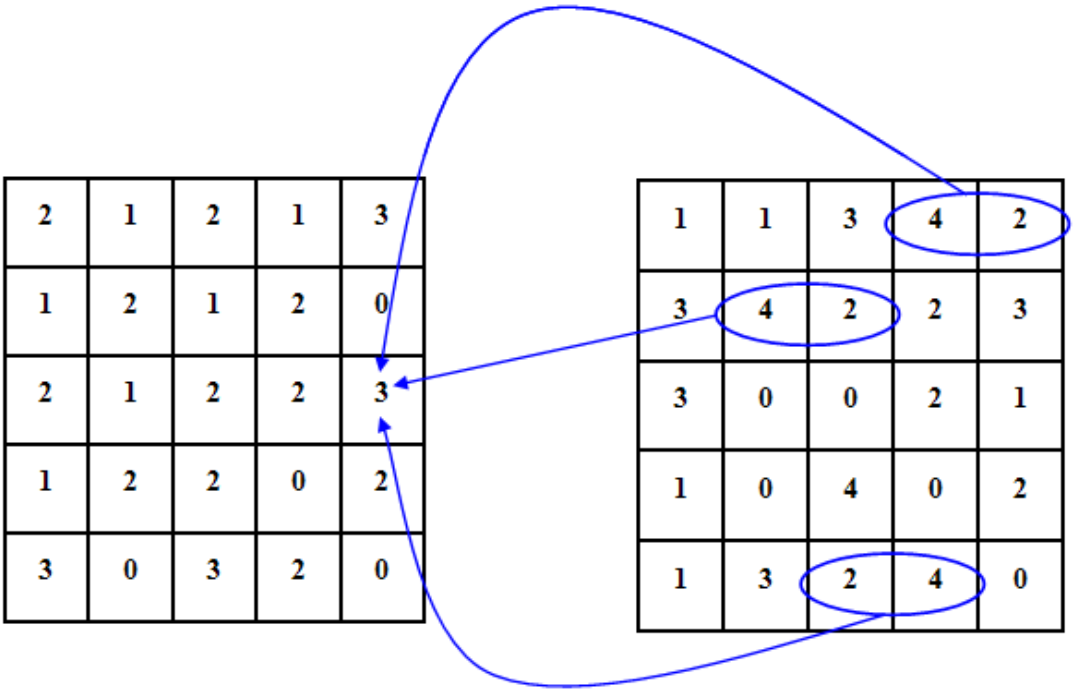

Figure 2.4: GLCM of the image in horizontal direction. Matrix to the left is the GLCM and to the right is the 5×5 original image

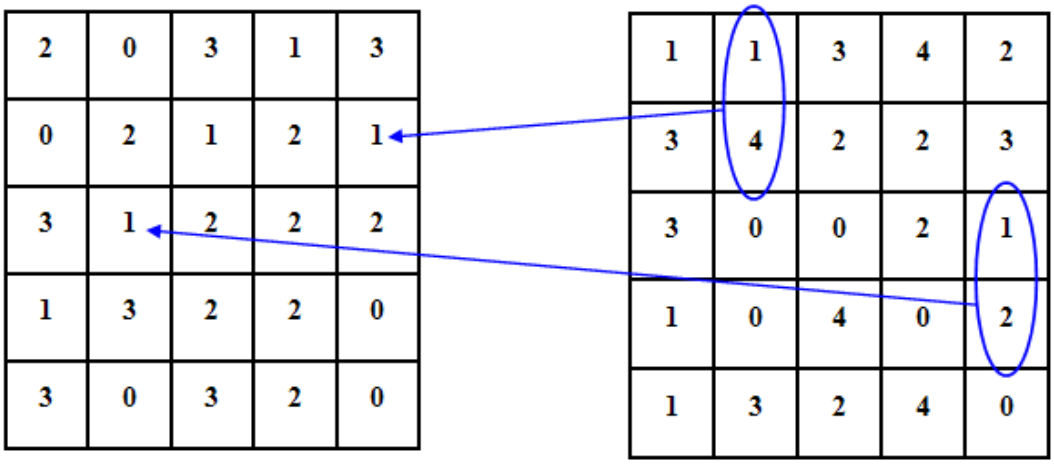

Figure 2.5: GLCM of the image in vertical direction. Matrix to the left is the GLCM and to the right is the 5×5 original image

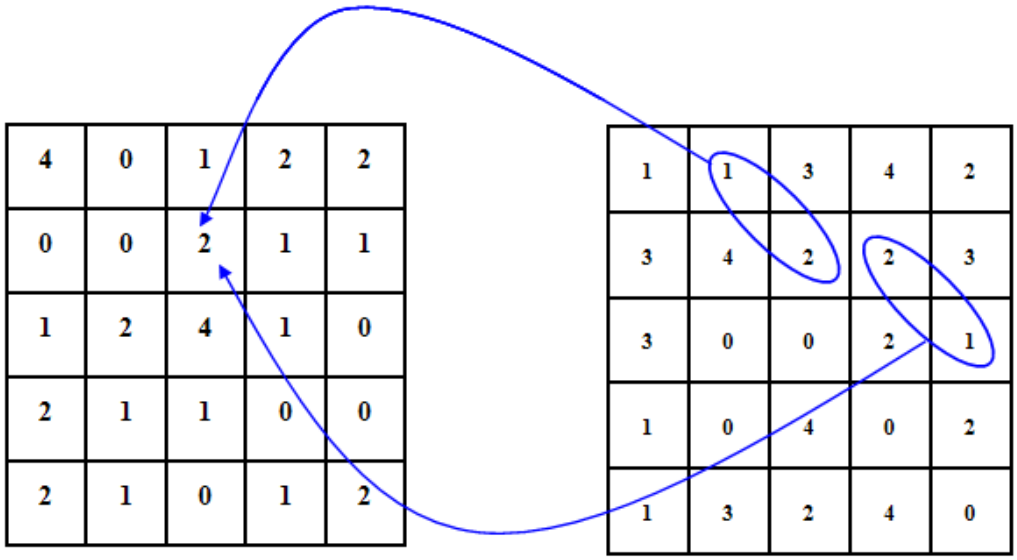

Figure 2.6: GLCM of the image in left diagonal direction. Matrix to the left is the GLCM and to the right is the 5×5 original image

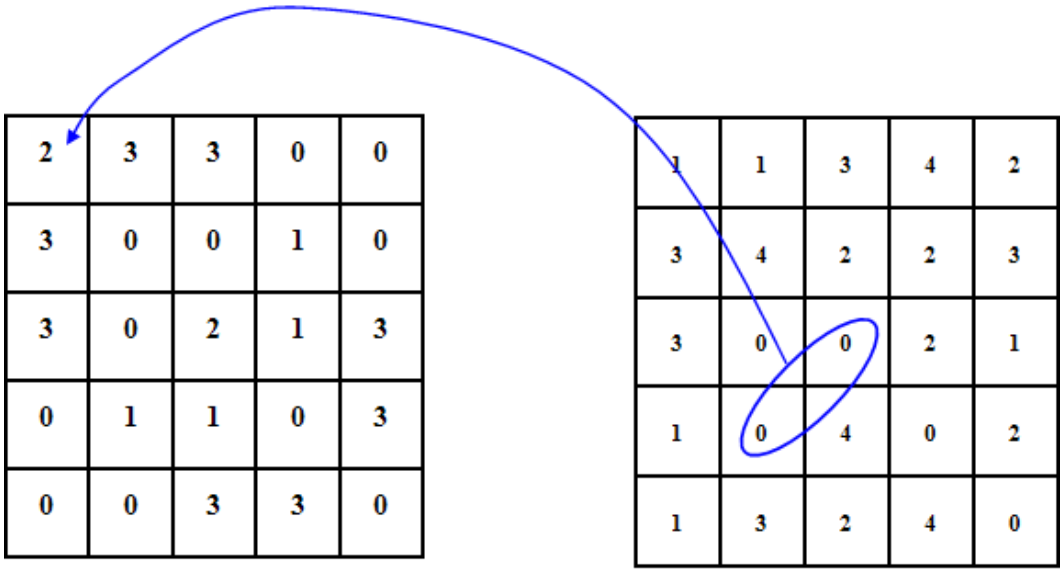

Figure 2.7: GLCM of the image in right diagonal direction. Matrix to the left is the GLCM and to the right is the 5×5 original image

2.8 Colour Models

Various colour representations are used in colour image processing. Colour can be represented by a RGB space, where colours are represented by their red, green and blue component in an orthogonal Cartesian space. From R, G,B, representation, different kinds of colour spaces are derived using linear and nonlinear transformation. Any of the colour spaces can be utilized for image segmentation. However selecting the best colour space for particular types of images is still a challenging problem. RGB is the commonly used model for the television system and pictures acquired by digital cameras. But for natural scene segmentation and analysis RGB is not considered as the good one due to high correlation among R, G and B components. High correlation here means that if intensity changes, all the three components will change accordingly. Both RGB and HIS (or HSV) spaces are not perceptually uniform. From R, G, B representation , other kinds of colour representations are derived by using either linear or nonlinear transformations. The following are the colour spaces, which can be found by linear transformations.

2.8.1 YIQ

In this model each colour is represented in terms of a luminance component (Y) and two chrominance or colour components: inphase (I) and quadrature (Q) component. United States commercial TV broadcasting (NTSC) system utilizes this model. All the video information needed by a monochrome TV monitor is rendered by Y component. The model is obtained from RGB model by a linear transformation

$$\begin{pmatrix} Y \\ I \\ Q \end{pmatrix} = \begin{pmatrix} 0.299 & 0.587 & 0.114 \\ 0.596 & -0.275 & -0.321 \\ 0.212 & -0.523 & 0.311 \end{pmatrix} \begin{pmatrix} R \\ G \\ B \end{pmatrix} \tag{2.7}$$

The fact that the luminance and chrominance component can be processed separately is the advantage of this model.Hue and saturation of the image are described jointly by components I and Q. Y component is used in edge detection.

2.8.2 YUV

This colour space representation is being used by European TV system. This is obtained from RGB model by

$$\begin{pmatrix} Y \\ U \\ V \end{pmatrix} = \begin{pmatrix} 0.299 & 0.587 & 0.114 \\ -0.147 & -0.289 & 0.437 \\ 0.615 & -0.515 & -0.100 \end{pmatrix} \begin{pmatrix} R \\ G \\ B \end{pmatrix} \tag{2.8}$$

where 0≤R≤1, 0≤G≤1, 0≤B≤1.

2.8.3 Normalized RGB (Nrgb)

The normalized RGB colour space is given by

$$r = R/(R+G+B)$$
$$g = G/(R+G+B)$$
$$b = B/(R+G+B)$$

While performing colour image segmentation, it is necessary to make the colours independent, on the change in lighting intensities. An effective method is the use of normalized RGB colour space. This is because, as r+g+b =1, if two components are given the third component can be determined.

Another normalized colour space is defined in [44] and is given by

$$Y = c_1R + c_2G + c_3B$$
$$T_1 = \frac{R}{R+G+B}$$
$$T_2 = \frac{G}{R+G+B}$$

where $c_1 + c_2 + c_3 = 1$, c_1,c_2 and c_3 are constants and they are combined to produce illumination of image pixel. T_1 and T_2 are determined by the share of RGB components and hence symbolize the very colour information of an image, but are independent of the brightness of the image.

2.8.4 HSI

The HSI (hue-saturation-intensity) system is another commonly used colour spaces in image processing. In this colour space the colour information is represented by hue and saturation values and intensity describes the brightness of an image. HSI coordinates in terms of R, G and B values is given by

$$H = arctan\left(\frac{\sqrt{3}(G-B)}{(R-G)+(R-B)}\right)$$
$$I = \frac{R+G+B}{3}$$
$$S = 1 - \frac{min(R,G,B)}{I}$$

The potentiality of this system is that it can represent the colours of the human perception. To segment the objects using this colour space, segmentation algorithms can be applied to hue component only. But the difficulty with this is to transform these back to RGB values.

2.8.5 CIE spaces

CIE (International commission on illumination) [45] colour models are highly influential systems for measuring colour or distinguishing between colours. It has three primaries denoted as $X, YandZ$. The values of X,Y and Z can be computed as a linear transformation from RGB tristimulus coordinates as

$$\begin{pmatrix} X \\ Y \\ Z \end{pmatrix} = \begin{pmatrix} 0.607 & 0.174 & 0.200 \\ 0.299 & 0.587 & 0.114 \\ 0.000 & 0.066 & 1.116 \end{pmatrix} \begin{pmatrix} R \\ G \\ B \end{pmatrix}$$

Once the tristimulus coordinates are known CIE spaces can be developed. The two distinctive ones are $CIE(L*a*b*)$ space and $CIE(L*u*v*)$ space. $CIE(L*a*b*)$

is defined as

$$L^* = 116\left(\sqrt[3]{\frac{y}{y_0}}\right) - 16$$
$$a^* = 500\left[\sqrt[3]{\frac{X}{X_0}} - \sqrt[3]{\frac{Y}{Y_0}}\right]$$
$$b^* = 200\left[\sqrt[3]{\frac{Y}{Y_0}} - \sqrt[3]{\frac{Z}{Z_0}}\right]$$

Where (X_0, Y_0, Z_0) are X, Y, Z values for the standard white.
Here $\frac{Y}{Y_0} > 0.01, \frac{X}{X_0} > 0.01 and \frac{Z}{Z_0} > 0.01$
$CIE(L^*u^*v^*)$is defined as:

$$L^* = 116\left(\sqrt[3]{\frac{y}{y_0}}\right) - 16$$
$$u^* = 13L^*(u^1 - u_0)$$
$$v^* = 13L^*(v^1 - v_0)$$

Where $\frac{y}{y_0} > 0.01$, y_0, u_0 and v_0 are the values for standard white.

$$u^1 = \frac{4x}{x + 15y + 3z} \qquad and$$
$$v^1 = \frac{6y}{x + 15y + 3z}$$

2.8.6 Munsell Colour system

Munsell Colour system uses three attributes of colour perception, which are Munsell hue, value and chroma. There are five colours regarded as the major hue. They are red(r), yellow(y), green(g), blue(b) and purple(p). Combinations of colours:YR, GY, BG, PB and RP are half way hues. Munsell value (v) describes the lightness of a colour. The value of black as 0 and that of white as 10.
Relationship between v and luminance Y is

$$Y = 1.2219v - 0.23111v^2 + 0.23951v^3 - 0.021009v^4 + 0.0008404v^5 \qquad (2.9)$$

Chroma (C) is similar to the saturation component in the CIE representation, which describes purity of colour.

2.8.7 Ohta Colour Space

At each step of the recursive region splitting, new colour features are calculated by using a transform "Karhunen-Loeve transformation" of R, G and B. It is applied to eight kinds colour pictures analyzed over 100 colour features, and a set of effective colour features can be found by

$$I_1 = (R + G + B)/3$$
$$I_2 = (R - B)/2$$
$$I_3 = (2G - R - B)/4$$

Comparing I_1, I_2, I_3 with 7 other colour spaces, i.e., RGB, YIQ, HIS, $Nrgb$, $CIEXYZ$, $CIE, L^*a^*b^*$ and $CIEL^*a^*b^*$, it is seen that I_1, I_2, I_3 was effective in terms of quality of segmentation and computational complexity of the algorithm. Major problem in linear colour spaces is (i) There is high correlation of three components, by which three components are dependent upon each other and associate strongly. (ii) These spaces are very difficult to discriminate highlights, shadows and shading. So if these spaces are used in segmentation, it is performed in a 3-D spaces, usually one component at a time.

Chapter 3

Unsupervised Segmentation of Colour Textured Images using Gaussian Markov Random Field Model and Genetic Algorithm

3.1 Introduction

Segmentation of coloured textured images is one of the fundamental operations in the arena of colour image analysis. Image data at moderate and coarse spatial resolutions can be differentiated based on the spectral reflectance patterns alone. But increase in the size of the objects with high spatial resolution imagery, brings in the texture effects and thus the role of texture assumes more significance. This is mainly witnessed in natural scene images as well as remotely sensed multispectral images. This limits the potential of spectral information and thus the contextual classifiers utilizing both spatial and spectral information gain importance. Often the model based approaches have been adhered to obtain proper segmentation of colour textured images. In this regard, the segmentation problem is cast as unsupervised mode of segmentation. In case of unsupervised method of segmentation, the number of classes, model parameters as well as image labels are unknown. Whereas the problem becomes partially unsupervised when the number of classes are known. In this chapter Gaussian Markov random field model (GMRF) as proposed by Panjwani and Healey [31] has been employed to formulate the unsupervised segmentation problem. In this GMRF model within color planes and

between color bands interaction is taken into account. In MRF based segmentation, the most popular criterion for optimality has been maximizing *a posteriori* probability (MAP) distribution criterion. Simulated annealing (SA) and iterated conditional modes (ICM) algorithm are two unremarkably used methods for pixel labeling among the existing MAP criterion algorithms. SA can converge to global optimum, but suffers from intensive computation. On the other hand, the results obtained from ICM heavily depend on initialization and hence there is a probability of trapping into local maxima. Hence it suffers from inaccurate estimations. Genetic algorithm (GA) has the advantage of coming out of local optima and converges in global optima. Utilizing this property Tseng and Lai [33] have employed GA to provide better initialization for the ICM algorithm. In this chapter we have employed the hybridization of GA and GMRF model for segmentation of colour textured images.

3.2 Gaussian Markov Random Field Model

The Gaussian Markov random field (GMRF) model being examined is a special case of Markov random field model(MRF) where the pixel value at location (i, j) statistically depends on the neighbouring pixels of the representing component together with the neighbouring pixels of the other components. This signifies that the model considers spatial interactions within each colour component and the interactions between different components. The image is represented on a rectangular lattice $S = M \times N$ with p number of bands.

Let $X(i, j) = [x_1(i, j)x_2(i, j)..x_p(i, j)]$ represent a colour vector at location (i,j) in a textured region R. Let μ_1, μ_2 . . μ_p denote the mean colour intensities. It is assumed that the colour vector at location (i, j) represents the linear combination of the colour components of neighbouring pixels and the additive Gaussian noise. Let e_1, e_2 . . e_p represent the spatial interaction of the pixels and v_{xy} be the expected value of $e_x e_y$. x, y takes on the values from 1 to p. Let ϕ_{xy} be the associated model parameters and Σ be the correlation matrix.

The spatial interaction of the colour pixels is defined as

$$\begin{aligned} e_1(i,j) = (x_1(i,j) - \mu_1) &- \sum_{(m,n)\in N_{11}} \phi_{11}(m,n)\big(x_1(i+m,j+n) - \mu_1\big) \\ &- \sum_{(m,n)\in N_{12}} \phi_{12}(m,n)\big(x_2(i+m,j+n) - \mu_2\big) - \cdots \\ &- \sum_{(m,n)\in N_{1p}} \phi_{1p}(m,n)\big(x_p(i+m,j+n) - \mu_p\big) \end{aligned} \tag{3.1}$$

Similarly it is defined for $e_2(i,j)$, $e_3(i,j)$ . . $e_p(i,j)$. The generalized form is given by

$$\begin{aligned} e_p(i,j) = (x_p(i,j) - \mu_p) &- \sum_{(m,n)\in N_{p1}} \phi_{p1}(m,n)\big(x_1(i+m,j+n) - \mu_1\big) \\ &- \sum_{(m,n)\in N_{p2}} \phi_{p2}(m,n)\big(x_2(i+m,j+n) - \mu_2\big) - \cdots \\ &- \sum_{(m,n)\in N_{pp}} \phi_{pp}(m,n)\big(x_p(i+m,j+n) - \mu_p\big) \end{aligned} \tag{3.2}$$

where N_{xy} denote the neighbouring pixels. This implies that the pixel considered is in x component and the neighbours are from y colour component. If $x = y$, then the neighboring pixels will correspond to the same colour component. Otherwise the neighbouring pixels will be from other components. The spatial interaction is graphically represented in Figure 3.1.

The correlation matrix is estimated as follows

$$\sum = \begin{pmatrix} v_{11} & v_{12} & . & . & v_{1p} \\ v_{21} & v_{22} & . & . & v_{2p} \\ . & . & . & . & v_{1p} \\ . & . & . & . & v_{1p} \\ v_{p1} & v_{p2} & . & . & v_{pp} \end{pmatrix} \tag{3.3}$$

The expected value v_{kl} is represented by,

$$v_{kl} = E[e_k e_l] = \frac{1}{M_R} \sum_{(i,j)\in R} e_k(i,j) e_l(i,j) \tag{3.4}$$

Having described all the terms, the probability density function of X(i,j) is obtained by,

$$P\left(X(i,j) \mid R\right) = \frac{1}{\left((2\pi)^P \mid \sum \mid\right)^{\frac{1}{2}}} \exp\left\{\frac{-1}{2}\left(e_1(i,j)e_2(i,j)...e_p(i,j)\right)\sum^{2}\left(e_1(i,j)e_2(i,j)...e_p(i,j)\right)^t\right\} \tag{3.5}$$

3.3 Parameter Estimation

Given the statistical model, maximum likelihood estimation method estimates the parameters of the model by maximizing the probability (likelihood) of the sample data. It is regarded as one of the most robust methods. In this work the maximum likelihood method is applied to formulate maximum likelihood estimates of the parameters of the GMRF model. For the model, the product of conditional probability densities of individual pixels of a region is given by

$$\prod_{(i,j)\in R} \frac{1}{\left((2\pi)^p \mid \sum_R \mid\right)^{\frac{1}{2}}} \exp\left\{\frac{-1}{2}\left(e_1(i,j)e_2(i,j)...e_p(i,j)\right)\sum_{R}\left(e_1(i,j)e_2(i,j)...e_p(i,j)\right)^t\right\} \tag{3.6}$$

By maximizing the above function the parameter ϕ_{xy} is estimated by solving a set of linear equations. Let,

$$q_p(i,j) = x_p(i,j) - \mu_p \qquad and$$

$$q_{p,mn}(i,j) = x_p(i+m, j+n) - \mu_p$$

Then the parameters are found by solving the following equation,

$$\sum_{(i,j)\in R} \begin{pmatrix} q_{1,10}^2 & q_{1,10}q_{1,01} & \cdots & q_{1,10}q_{p,10} & \cdots \\ \cdots & \cdots & \cdots & \cdots & \cdots \\ q_{1,mn}q_{1,10} & q_{1,mn}q_{1,01} & \cdots & q_{1,mn}q_{p,10} & \cdots \\ \cdots & \cdots & \cdots & \cdots & \cdots \\ q_{p,10}q_{1,10} & q_{p,10}q_{1,01} & \cdots & q_{p,10}^2 & \cdots \\ \cdots & \cdots & \cdots & \cdots & \cdots \\ q_{p,mn}q_{1,10} & q_{p,mn}q_{1,01} & \cdots & q_{p,mn}^2 & \cdots \end{pmatrix} \begin{pmatrix} \phi_{11}(1,0) \\ \cdots \\ \phi_{11}(m,n) \\ \cdots \\ \phi_{1p}(1,0) \\ \cdots \\ \phi_{1p}(m,n) \end{pmatrix} = \sum_{(i,j)\in R} \begin{pmatrix} q_1 q_{1,10} \\ \cdots \\ q_1 q_{1,mn} \\ \cdots \\ q_1 q_{p,10} \\ \cdots \\ q_1 q_{p,mn} \end{pmatrix} \tag{3.7}$$

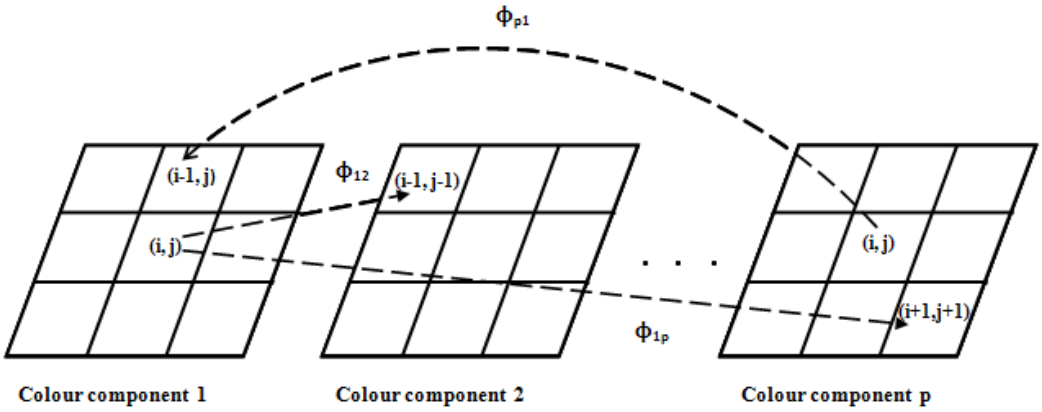

Figure 3.1: Spatial interaction between the colour components

3.4 Average Spatial Filtering

An important application of spatial averaging is to blur an image with an intention to find a gross representation of objects of interest, such that the intensity of small objects blends with the background and larger objects become blob like and easy to detect. In a textured image, an image will be comprised of texture primitives called texels. The type of texture depends on the size of texels. A fine texture results when the texels are small and tonal differences between the texels are large. A coarse texture is an assemblage of large texels. With the application of average filter, the colour of the texture region can be roughly known using the colours of nearby texels. The value of each pixel in the image is substituted by the average of gray values in the neighbourhood as defined by the convolution mask thus reducing the sharp transitions of gray values in the image. Similar to the random noise, which typically consists of sharp transitions, a texture image can be viewed as an image with sharp transitions. This is justified by the fact that a texture is a function of the spatial variation in pixel intensities over a region. Hence by applying an average filter produces a coarse segmented result. The centres of all these regions will be utilized in the following segmentation.

3.5 Genetic Algorithm

Genetic Algorithm (GA) holds a fixed population of solutions over the search space on which the different operations of GA are performed. Following are the operations carried out,

A. *Chromosome representation:*

A chromosome may be encoded with binary, integer or real numbers. In our work each of the values of the colour vector $X(i,j) = [x_1(i,j)x_2(i,j)..x_p(i,j)]$ representing the components of a pixel is taken as an individual or chromosome. The representation is as shown in Figure 3.2.

B. *Population initialization:*

Population is initialized by using the result of average spatial filtering. One of the individual is taken from the result where as the other individuals are generated randomly.

C. *Fitness computation:*

A fitness function is one that dictates the optimality of a chromosome so that

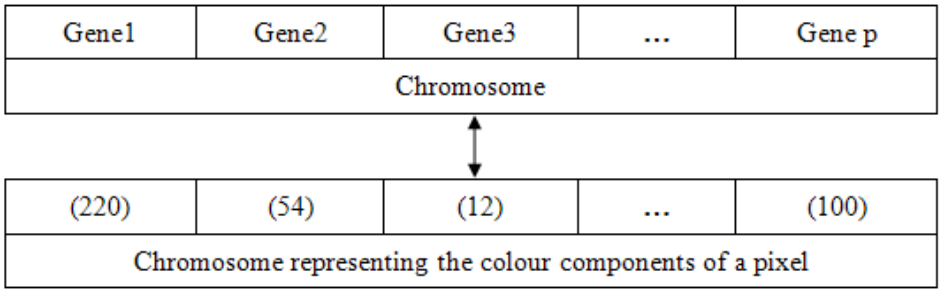

Figure 3.2: Representation of a Chromosome

specific chromosome may be stratified versus all the other chromosomes. Since the colour vector which maximizes the conditional probability density has to be determined, the fitness function is same as defined in Eq. 3.8

$$F = P\left(X(i,j)|R|\right) = \frac{1}{((2\pi)^p \mid \sum |)^{\frac{1}{2}}} \times \exp\left\{\frac{-1}{2}\left(e_1(i,j)e_2(i,j)...e_p(i,j)\right)\frac{1}{\sum}\left(e_1(i,j)e_2(i,j)...e_p(i,j)\right)^t\right\} \tag{3.8}$$

D. *Selection*

Once the fitness of every individual or the chromosome is determined, the next important step is the breeding process where fresh filtered individuals or off springs are created. The initial step of the breeding process is the Selection operation. A proportion of the existing population is selected to breed a new generation during each successive generation. The various selection methods include Roulette Wheel selection, Random selection, Rank selection Tournament selection and Boltzmann selection. Here we have considered Roulette Wheel selection.

E. *Cross Over*

Crossover being the second stair of the breeding phenomena allows solutions (chromosomes) to exchange information and produce new chromosomes. Two parents selected through the roulette wheel selection criteria mentioned above, participate in crossover. A cross site is chosen randomly along the string length and the values are interchanged after that cite, to produce children. The crossover is accomplished with a probability μ_c. The existing crossover techniques constitute single point crossover, two point crossover, multi point crossover, uniform crossover and three parent crossover. Single point cross over procedure by stochastic means is followed in this work.

Example:

P1: (51.0) (67.0) | (78.0) (98.0)

P2: (212.0) (86.0) | (133.0) (19.0)

P1 and P2 represent parent1 and parent2. The line shown is the point where crossover takes place. The genes after that position are exchanged to produce children.

Child1: (51.0) (67.0) | (133.0) (19.0)

Child2: (212.0) (86.0) | (78.0) (98.0)

F. *Mutation*

Mutation is an operation employed to prevent the possibility of the algorithm to get trapped in a local minima. It makes for the purpose of retrieving the lost genetic information. The strings are subjected to mutation after the crossover operation and this makes the third step of breeding process. Biological mutation refers to a sudden change in the characteristics of the gene. Following the same idea mutation here refers to the change in the value of the gene. For binary representation of the string, mutation comprises in flipping the value of each gene with a mutation probability μ_m. In case of real or integer value, a gene is replaced with a random number from the corresponding solution area which is known as random mutation. One more way is to stochastically changing a gene over time by adding or subtracting a random number which is acknowledged as dynamic mutation. In this scheme random mutation strategy is followed.

G. *Termination Criteria*

The execution is terminated with maximum number of iterations. An elite chromosome preserved in a location outside the population with maximum fitness contains the components of the final colour vector of the region.

3.6 Hybridization of GA and GMRF for colour texture image segmentation

A. Iterated conditional modes (ICM) algorithm was proposed by Besag [8] as a computationally feasible substitute to MAP estimate. Local convergence based scheme is followed for rapid convergence in order to obtain the optimal solution. Iterated conditional modes (ICM) algorithm is adopted as local convergent algorithm. The steps of ICM algorithm are given as below,

1. Find out number of iterations N, the neighborhood system and model

parameters for energy function described in Eqn. 3.8

2. Initialize the image of configuration w for each pixel.
3. Evaluate the energy E of the configuration.
4. Disturb the system reasonably with Gaussian disturbance

- Compute the new energy E^* of the newly disturbed system and measure the change in the energy $\delta E = E^* - E$.

5. If $\delta E < 0$, accept the disturbed system as new configuration, else retain the original configuration
6. Repeat steps $3 - 6$, till the number of iterations are completed.

B. As already stated in sec 3.1 ICM algorithm is sensitive to initialization condition for proper segmentation. To overcome this bottleneck, genetic algorithm is hybridized with ICM algorithm and employed in GMRF model for better initialization and to improve the performance of segmentation. Using this hybrid method, the fast convergence of ICM algorithm and global exploration of GA are achieved simultaneously. The steps of proposed GMRF-GA-ICM algorithm are described as follows.
GMRF-GA-ICM Algorithm:

- A coarse segmentation is performed to get the initial regions using average spatial filtering and K-means algorithm. The result of the average filter is given as the input to K-means algorithm to perform clustering. This helps in approximately labelling the pixels, to find the mean value of the regions and to reduce the amount of time required in MRF based iterative process.
- The initialization of ICM algorithm is performed using genetic algorithm as follows
  The spectral vector $X(i,j) = \{x_1(i,j)x_2(i,j)...x_p(i,j)\}$ representing the spectral components of a pixel is encoded as an individual. The result of the coarse segmentation obtained by average filter and K-means

algorithm is taken as the individual in the population initialization process and the remaining individuals are generated randomly. Each individual is then evaluated using the fitness function defined in Eq. 3.8 and the better individuals are selected to raise the next generation using the selection procedure as mentioned in section 3.5. This is followed by crossover and mutation operations to get the better solutions. The procedure is continued till the maximum number of generations is accomplished. The individual with the highest fitness is used to give the initial label for ICM algorithm.

- Then the ICM algorithm is executed to produce the final segmented image.

C. Control parameters: The performance of overall segmentation approach depends on the parameters namely population size, crossover and mutation probability and the number of iterations of ICM algorithm. The size of the population governs strongly the performance of GAs. With the small sized population the evaluation cost of GA is reduced due to insufficient samples in the search space. GA can get better solutions if the population size is large because of the presence of more characteristic solutions over the search space. But this takes more computations which is an hindrance to faster convergence rate. High crossover probability may result in unstable solutions and if it is low GA may become idle to search for new solutions. Furthermore, the search process turns into a haphazard-like process if the mutation probability is too high. Hence it should be seen that the values of the parameters are also optimal. After having acknowledged all these facts population size of 100 with 100 number of generations, Crossover probability of 0.8, Mutation probability of 0.1 and 10 number of iterations of ICM algorithm were considered for simulation.

3.7 Simulation and Results

In simulation, synthetic textured images and natural scene images are considered to validate the proposed algorithm. Coloured textured images consisting of 2, 3 and 4 classes are considered for the simulations. The images used for experimentation are taken from "http://www.visual28.com", "http://www.imageafter.com/", "http://www.cgtextures.com/" and "http://www.sketchpad.net".

Figure 3.3(a) shows a two class synthetic colour textured image. The size of the image is 130×130. As stated in the previous sections average spatial filtering and K-means algorithm is applied in order to speed up the coarse segmentation. Then the image is initialized using GA followed by execution of ICM algorithm. The model parameters ϕ_{xy} are obtained as described in section 3.3. The performance of the proposed technique is compared with that of simulated annealing algorithm and ICM algorithm using GMRF model.

Figure 3.3(a) shows a 2 class synthetic textured image of size (130×130). Figure 3.3(b) shows the ground truth image and Figures 3.3(c), 3.3(d) and 3.3(e) show the segmented images using SA algorithm, ICM algorithm and using GMRF-GA-ICM algorithm respectively. Tables 3.1, 3.2 and 3.3 show the GMRF model parameters for the spatial interaction of the color components. Table 3.4 depicts performance comparison of the three techniques with performance index as misclassification error and computation time of different techniques. It is found from the table that SA algorithm obtains satisfactory results but computation time is high which is 56 seconds. ICM algorithm converges very quickly in only 10 seconds but fails to give accurate results. The proposed algorithm which utilizes the property of global optimization of GA for initializing the ICM algorithm succeeds in converging in less time than SA and giving better segmentation results as that of SA. It converges only in 30 seconds. The misclassification error is found to be 7.04% in case of SA, 16.34% in case of ICM and 6.31% in case of GMRF-GA-ICM algorithm respectively.

Similarly, the proposed technique is examined for a two class real image. Fig-

ure 3.4(a) shows a two class real image of size (175×170). Figure 3.4(b) represents the ground truth image. Figures 3.4(c), 3.4(d) and 3.4(e) show the segmented images using SA, GMRF-ICM and GMRF-GA-ICM algorithms respectively. Again it is found that the proposed algorithm is better in terms of both accuracy and time complexity.

Similarly a three class synthetic textured image of size (180×154) is shown in Figure 3.5(a). The GMRF model parameters are shown by the Tables 3.6, 3.7 and 3.8. Again, the segmented results using SA, GMRF-ICM and GMRF-GA-ICM algorithms are shown in Figures 3.5(c), 3.5(d) and 3.5(e) respectively. It is observed that the proposed method performs better than GMRF-ICM as well as GMRF-SA algorithm. Misclassification error and time complexity are shown in Table 3.9.

The proposed method is tested also for a 4 class synthetic textured image. Figure 3.6(a) shows the 4 class synthetic textured image of size (200×200). The GMRF model parameters for the 4 class image are depicted in Tables 3.10, 3.11 and 3.12. Misclassification error and the time complexity is shown in Table 3.13. Few more results are shown in Chapter 4 in comparison with the new scheme proposed in chapter 4.

3.8 Conclusion

This chapter addresses the problem of color textured image segmentation in unsupervised framework. Color textured image segmentation using compound Gaussian Markov Random Field (GMRF) model hybridized with genetic algorithm is proposed. Within and between color plane spatial interaction is considered as the pixel value at location (i, j) statistically depends on the neighbouring pixels of the representing component together with the neighbouring pixels of the other components. The image labels are estimated using MAP criteria. Iterated conditional modes (ICM) algorithm is used for MAP estimation of image labels. The global

convergence property of GA is exploited to provide better initialization condition for ICM algorithm. The proposed method is tested for two class, three class and four class color textured images and found that it performs better than ICM and SA algorithm in terms of accuracy and computational time.

Hybrid GMRF-GA-ICM method obtains better segmentation due to the fact that firstly the model takes into account not only spatial interaction within each of the color bands but also the interaction between the different bands. Secondly it uses GA for the initialization of the ICM algorithm. It has the advantage of combining the fast convergence of ICM and global exploration of GA.

(a) Original Image

(b) Ground truth

(c) GMRF-SA

(d) GMRF-ICM

(e) GMRF-GA-ICM

Figure 3.3: Segmentation result of two class synthetic colour textured Image

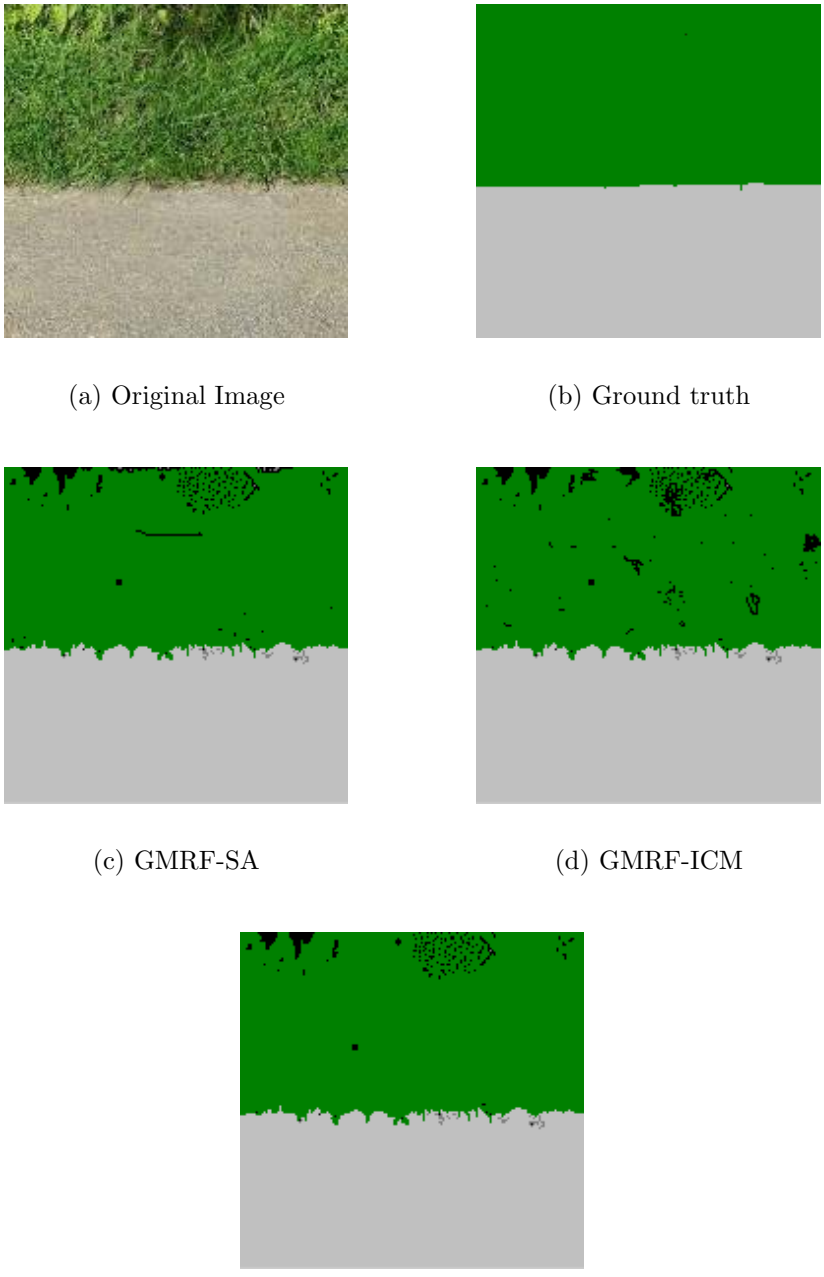

(a) Original Image

(b) Ground truth

(c) GMRF-SA

(d) GMRF-ICM

(e) GMRF-GA-ICM

Figure 3.4: Segmentation result of two class real textured image

Table 3.1: The GMRF parameters for the spatial interaction of the colour component 1 with the other colour components 2 and 3 for the image in Figure 3.3(a)

GMRF Parameter	Region1	Region2
$\phi_{11}(0,1)$	-0.0471	-0.0151
$\phi_{11}(0,1)$	-0.0354	-0.0334
$\phi_{11}(1,1)$	0.0464	0.0343
$\phi_{11}(1,-1)$	0.0508	0.0261
$\phi_{12}(1,0)$	-0.0354	-0.0334
$\phi_{12}(0,1)$	0.0261	0.0455
$\phi_{12}(1,1)$	0.1862	0.1475
$\phi_{12}(1,-1)$	0.061	0.0224
$\phi_{13}(1,0)$	0.0285	0.0864
$\phi_{13}(0,1)$	0.0173	0.0794
$\phi_{13}(1,1)$	0.1759	0.1354
$\phi_{13}(1,-1)$	0.0827	0.07

Table 3.2: The GMRF parameters for the spatial interaction of the colour component 2 with the other colour components 1 and 3 for the image in Figure 3.3(a)

GMRF Parameter	Region1	Region2
$\phi_{21}(1,0)$	0.0422	0.1055
$\phi_{21}(0,1)$	0.0109	0.0897
$\phi_{21}(1,1)$	-0.0188	-0.0412
$\phi_{21}(1,-1)$	0.0637	0.0129
$\phi_{22}(1,0)$	0.0129	-0.0462
$\phi_{22}(0,1)$	-0.0214	0.08214
$\phi_{22}(1,1)$	-0.0151	0.0473
$\phi_{22}(1,-1)$	0.0692	0.02631
$\phi_{23}(1,0)$	0.0224	0.0637
$\phi_{23}(1,0)$	-0.0462	0.0224
$\phi_{23}(1,1)$	-0.0137	0.1862
$\phi_{23}(1,-1)$	0.1264	0.0847

Table 3.3: The GMRF parameters for the spatial interaction of the colour component 3 with the other colour components 1 and 2 for the image in Figure 3.3(a)

GMRF Parameter	Region1	Region2
$\phi_{31}(1,0)$	0.0182	0.2052
$\phi_{31}(0,1)$	-0.4037	0.0789
$\phi_{31}(1,1)$	0.0654	0.0724
$\phi_{31}(1,-1)$	0.0539	0.0965
$\phi_{32}(1,0)$	0.0271	0.3290
$\phi_{32}(0,1)$	0.0113	-0.0482
$\phi_{32}(1,1)$	0.0921	0.0675
$\phi_{32}(1,-1)$	0.0507	-0.0356
$\phi_{33}(1,0)$	0.2175	0.1921
$\phi_{33}(0,1)$	0.0462	0.0728
$\phi_{33}(1,1)$	0.06	0.0802
$\phi_{33}(1,-1)$	0.2551	0.0614

Table 3.4: Performance Comparison of various segmentation techniques for Figure 3.3(a)

Techniques	MCE in ٪	Time in sec.
SA	7.04	56
GMRF-ICM ONLY	16.34	10
GMRF-GA-ICM	6.31	30

Table 3.5: Performance Comparison of various segmentation techniques for Figure 3.4(a)

Techniques	MCE in ٪	Time in sec.
SA	5.14	53
GMRF-ICM ONLY	15.46	11
GMRF-GA-ICM	4.91	28

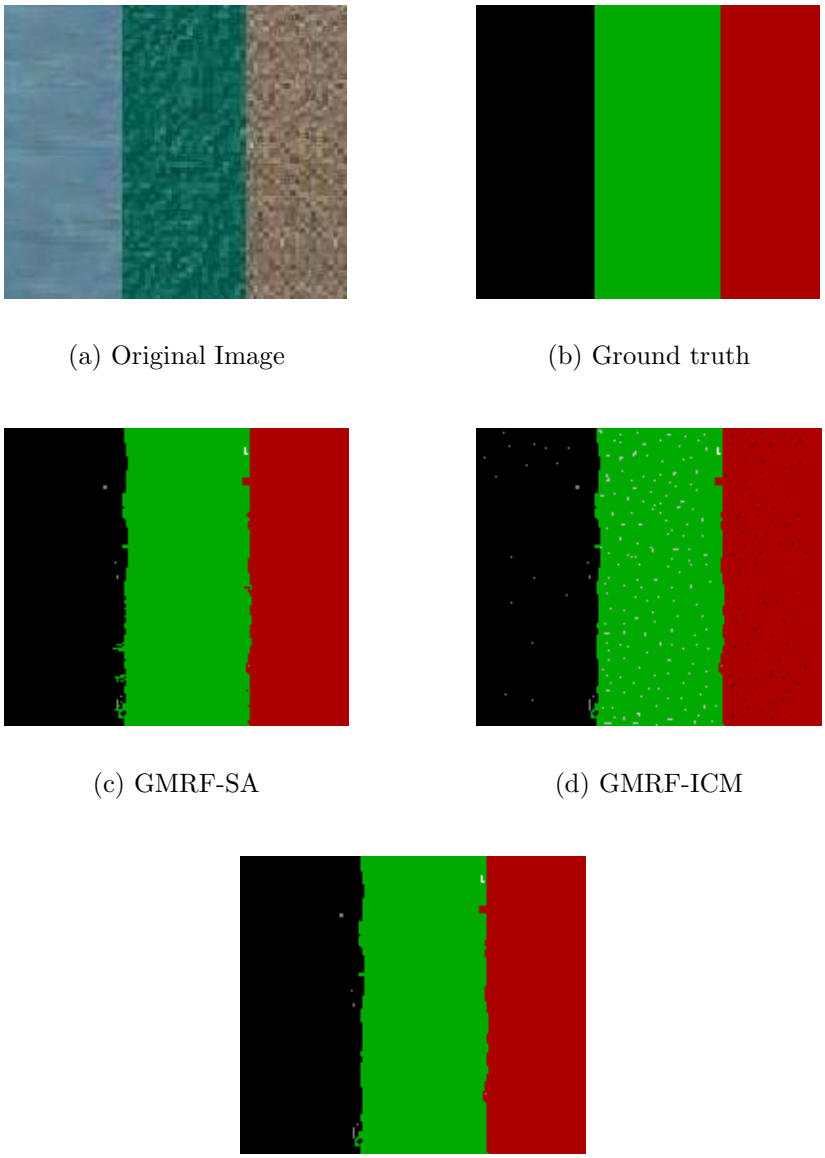

(a) Original Image

(b) Ground truth

(c) GMRF-SA

(d) GMRF-ICM

(e) GMRF-GA-ICM

Figure 3.5: Segmentation result of three class synthetic colour textured image

Table 3.6: The GMRF parameters for the spatial interaction of the colour component 1 with the other colour components 2 and 3 for the image in Figure 3.5(a)

GMRF Parameter	Region1	Region2	Region3
$\phi_{11}(0,1)$	0.0699	0.1275	0.058
$\phi_{11}(0,1)$	0.1102	0.2543	0.1114
$\phi_{11}(1,1)$	-0.2345	0.0967	0.0447
$\phi_{11}(1,-1)$	0.0158	0.6502	0.1094
$\phi_{12}(1,0)$	0.2031	0.0911	0.2081
$\phi_{12}(0,1)$	0.0619	-0.0914	0.2073
$\phi_{12}(1,1)$	0.1225	0.0418	-0.0061
$\phi_{12}(1,-1)$	0.1479	0.0355	0.0034
$\phi_{13}(1,0)$	0.0619	0.018	0.0017
$\phi_{13}(0,1)$	0.0256	0.1609	0.0175
$\phi_{13}(1,1)$	0.0098	-0.0832	0.2165
$\phi_{13}(1,-1)$	0.0902	0.1067	0.2649

Table 3.7: The GMRF parameters for the spatial interaction of the colour component 2 with the other colour components 1 and 3 for the image in Figure 3.5(a)

GMRF Parameter	Region1	Region2	Region3
$\phi_{21}(1,0)$	0.2045	0.1402	0.4125
$\phi_{21}(0,1)$	-0.2312	0.0117	0.2173
$\phi_{21}(1,1)$	-0.2081	-0.1401	0.0109
$\phi_{21}(1,-1)$	0.5031	0.1708	0.2456
$\phi_{22}(1,0)$	0.1038	0.1357	-0.1023
$\phi_{22}(0,1)$	0.048	0.213	0.0645
$\phi_{22}(1,1)$	-0.0901	0.0783	0.0594
$\phi_{22}(1,-1)$	0.4034	0.1897	0.0099
$\phi_{23}(1,0)$	0.0346	0.0178	0.2319
$\phi_{23}(1,0)$	0.0303	-0.3251	-0.0265
$\phi_{23}(1,1)$	0.0146	0.2206	-0.0740
$\phi_{23}(1,-1)$	-0.0462	0.0837	0.0629

Table 3.8: The GMRF parameters for the spatial interaction of the colour component 3 with the other colour components 1 and 2 for the image in Figure 3.5(a)

GMRF Parameter	Region1	Region2	Region3
$\phi_{31}(0,1)$	0.0127	0.3052	-0.1072
$\phi_{31}(0,1)$	0.0682	0.1487	0.3060
$\phi_{31}(1,1)$	-0.2037	-0.0454	-0.0674
$\phi_{31}(1,-1)$	-0.2251	-0.0973	0.0826
$\phi_{32}(1,0)$	0.0586	0.1225	0.0664
$\phi_{32}(0,1)$	0.0593	0.2049	-0.0908
$\phi_{32}(1,1)$	0.1213	0.07908	0.1061
$\phi_{32}(1,-1)$	-0.0385	0.2809	0.1009
$\phi_{33}(1,0)$	-0.3001	0.0713	0.1907
$\phi_{33}(0,1)$	0.2501	0.0439	0.0567
$\phi_{33}(1,1)$	0.0423	0.3285	0.0758
$\phi_{33}(1,-1)$	0.0905	0.1281	0.1073

Table 3.9: Performance Comparison of various Segmentation Techniques for Figure 3.5(a)

Techniques	MCE in ٪	Time in sec.
SA	4.04	44
GMRF-ICM ONLY	10.42	10
GMRF-GA-ICM	3.68	25

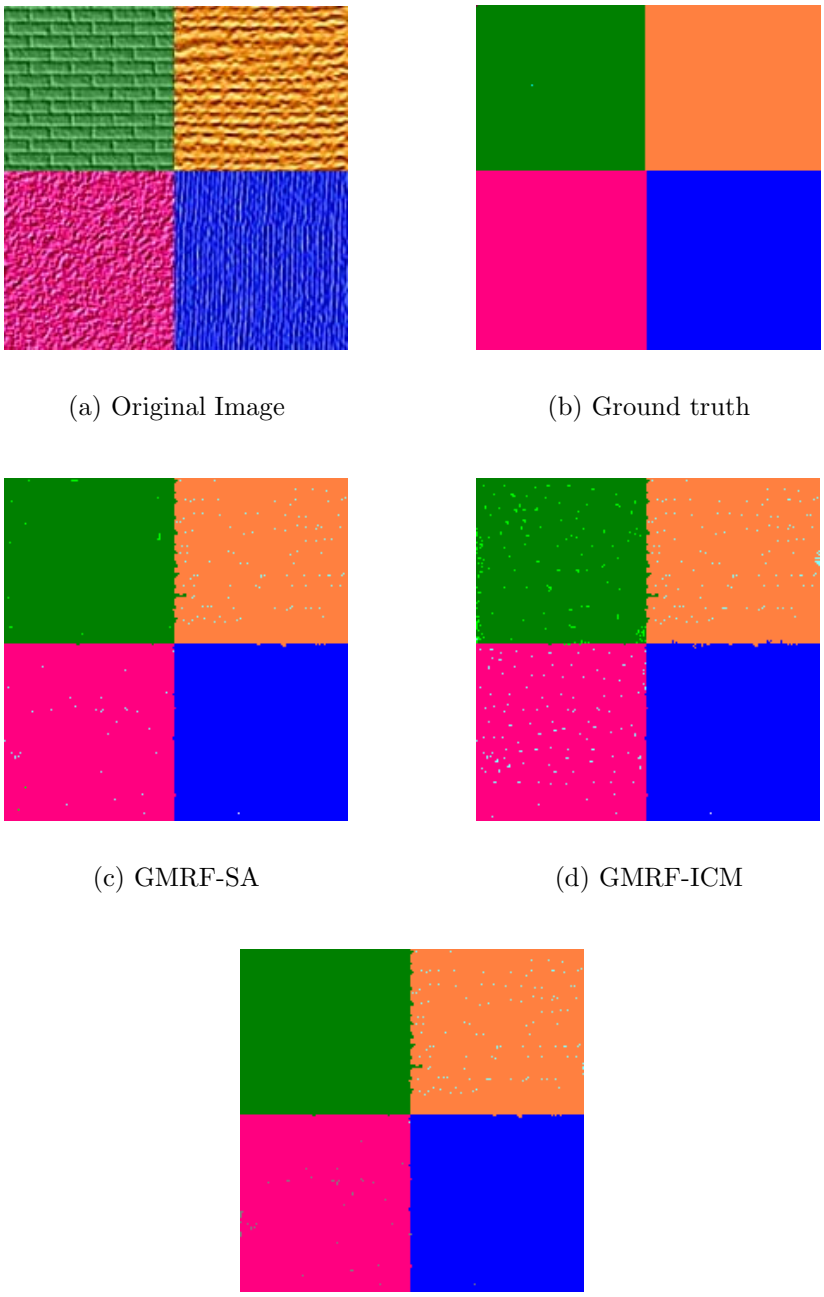

(a) Original Image

(b) Ground truth

(c) GMRF-SA

(d) GMRF-ICM

(e) GMRF-GA-ICM

Figure 3.6: Segmentation result of four class synthetic colored textured image

Table 3.10: The GMRF parameters for the spatial interaction of the colour component 1 with the other colour components 2 and 3 for the image in Figure 3.6(a)

GMRF Parameter	Region1	Region2	Region3	Region4
$\phi_{11}(0,1)$	0.0699	0.1275	0.058	0.2345
$\phi_{11}(0,1)$	0.1002	0.2543	0.1114	0.0967
$\phi_{11}(1,1)$	-0.0042	0.0343	0.0447	0.0158
$\phi_{11}(1,-1)$	0.0444	0.1524	0.094	0.0368
$\phi_{12}(1,0)$	0.0311	0.1184	0.051	0.1862
$\phi_{12}(0,1)$	0.0619	0.1654	0.0767	0.1225
$\phi_{12}(1,1)$	-0.0061	0.0418	0.0034	0.0098
$\phi_{12}(1,-1)$	0.0496	0.0355	0.0619	0.0832
$\phi_{13}(1,0)$	0.0119	0.018	0.0017	0.0063
$\phi_{13}(0,1)$	0.0256	0.1479	0.0175	0.2165
$\phi_{13}(1,1)$	0.0418	-0.0283	-0.0246	0.0649
$\phi_{13}(1,-1)$	0.0224	0.0637	0.0129	-0.0462

Table 3.11: The GMRF parameters for the spatial interaction of the colour component 2 with the other colour components 1 and 3 for the image in Figure 3.6(a)

GMRF Parameter	Region1	Region2	Region3	Region4
$\phi_{21}(1,0)$	0.05	0.0422	0.1055	-0.2312
$\phi_{21}(0,1)$	0.0895	0.1517	0.1274	0.5643
$\phi_{21}(1,1)$	-0.0188	-0.0412	0.0109	0.0897
$\phi_{21}(1,-1)$	0.0314	0.0708	0.0455	0.1351
$\phi_{22}(1,0)$	0.0368	0.1057	-0.0137	0.1862
$\phi_{22}(0,1)$	0.048	0.213	0.0645	-0.0309
$\phi_{22}(1,1)$	-0.0151	0.0473	0.0594	0.1897
$\phi_{22}(1,-1)$	0.0692	0.0303	0.079	0.2351
$\phi_{23}(1,0)$	0.0224	0.0637	0.0129	-0.0462
$\phi_{23}(1,0)$	0.0224	0.0637	0.0129	-0.0462
$\phi_{23}(1,1)$	0.0224	0.0637	0.0129	-0.0462
$\phi_{23}(1,-1)$	0.0224	0.0637	0.0129	-0.0462

Table 3.12: The GMRF parameters for the spatial interaction of the colour component 3 with the other colour components 1 and 2 for the image in Figure 3.6(a)

GMRF Parameter	Region1	Region2	Region3	Region4
$\phi_{31}(0,1)$	0.0387	0.0252	-0.0471	-0.0151
$\phi_{31}(0,1)$	0.0372	0.1227	0.0262	0.0473
$\phi_{31}(1,1)$	-0.0351	-0.0354	-0.0334	0.0129
$\phi_{31}(1,-1)$	-0.0619	0.1654	0.0767	0.1225
$\phi_{32}(1,0)$	0.0756	0.1876	0.0464	0.0343
$\phi_{32}(0,1)$	0.0231	0.0149	-0.0208	0.1713
$\phi_{32}(1,1)$	0.0717	0.0508	0.0261	0.0455
$\phi_{32}(1,-1)$	0.1075	0.1899	0.0909	-0.0151
$\phi_{33}(1,0)$	0.1764	0.1862	0.1475	0.5421
$\phi_{33}(0,1)$	0.0191	0.0439	0.061	0.0224
$\phi_{33}(1,1)$	0.1023	0.0285	0.08	0.0905
$\phi_{33}(1,-1)$	0.1351	0.0825	0.1033	0.213

Table 3.13: Performance Comparison of various segmentation techniques for Figure 3.6(a)

Techniques	MCE in ٪	Time in sec.
SA	4.04	69
GMRF-ICM ONLY	10.42	19
GMRF-GA-ICM	3.52	46

Chapter 4

MRF Model Based Image Segmentation of Color Textured Images using GLCM

In this chapter we propose a new method which blends the features of gray level co-occurrence matrix(GLCM) and Markov random field model(MRF) to segment colored textured images in Ohta colour space. The GMRF-GA model based technique proposed in Chapter 3 has few limitations. As discussed in Chapter 3 the method primarily depends on genetic algorithm for the initialization of the ICM algorithm. But GA does not assure to initialize the ICM algorithm each time the technique is executed. This is because of the fact that GAs are good at finding near optimal or acceptable good solutions but are not guaranteed to find the global optimum. Hence the method fails to yield better results in many of the trials and the results obtained in chapter 3 are the best among 15 to 20 trials. In order to overcome this difficulty and to improve the performance an attempt has been made to incorporate texture features of GLCM and MRF model together in one scheme to segment color textured images in Ohta color space. Texture can be defined as the variability in the tone with in a neighborhood, or the spatial relationships among the gray levels of neighboring pixels.

Among the approaches that have been followed to assess texture are the structural approach and statistical approach [10, 23, 46]. In the structural approach, a texture is considered as a structure composed of a large number of more or less ordered, similar elements or patterns with a certain rule of placement. The

complex problem associated with this approach is the extraction of such primitives. In statistical approach the stochastic properties of the spatial distribution of the gray levels in the image are characterized. Gray level co-occurrence matrices are among the simple and early statistical approaches to extract the textural features. Section 4.1 describes the GLCM textural measures and Markov random field model is described in section 1.2. The color models are used to represent different colors and the similarity in color is better interpreted in transformed spaces like HSV, YIQ, Ohta (I_1, I_2, I_3), CIE (XYZ, Luv, Lab) etc. In this chapter we have considered Ohta color model for image segmentation. The Ohta color space is an expression of the RGB color cube in terms of eigenvectors calculated over real scenes and produces better segmentations than in the RGB space since it segments real world imagery with respect to its principal components [38, 47].

4.1 Computation of Textural Measures using Gray Level Co-occurrence Matrix

Texture features based on GLCM are an efficient means to study the texture of an image. As already described in Chapter 2 , section 2.7, given the image composed of pixels each with an intensity, the GLCM is an illustration of how frequently different combinations of grey levels co-occur in an image. A GLCM denotes the second order conditional joint probability densities of each pixel gray level, which is the probability of occurrence of gray level i and grey level j within a given distance d and along the direction θ. Several statistical measures describing the texture have been deduced from GLCM. These second order statistics are calculated for all pair wise combinations of gray levels. Fourteen types of texture features have been defined by Haralick et. al. [23]. The depiction of the texture information is then extracted by these series of texture statistics computed from GLCM. In our study we have looked at eight conventional measures. Let N be the number of gray levels and $p(i, j)$ be the probability of co-occurrence of gray level i and gray level j, then the statistical measures are described as below

A. *Contrast (CON):*

Contrast defined as the difference between the highest and the smallest values of the adjacent set of pixels considered. The GLCM cumulous around the principal diagonal interprets a low contrast image and high contrast values mean a coarse texture.

$$CON = \sum_{i=0}^{N-1} \sum_{j=0}^{N-1} (i-j)^2 p(i,j) \tag{4.1}$$

B. *Dissimilarity (DIS):*

The heterogeneity of the gray levels is measured by dissimilarity. Over again the coarser textures are portrayed by higher values of dissimilarity.

$$DIS = \sum_{i=0}^{N-1} \sum_{j=0}^{N-1} Abs(i-j) p(i,j) \tag{4.2}$$

C. *Homogeneity (HOM):*

Homogeneity assesses image homogeneousness and for smaller difference between grey values it takes on larger values

$$HOM = \sum_{i=0}^{N-1} \sum_{j=0}^{N-1} \frac{p(i,j)}{\left[1+(i-j)^2\right]} \tag{4.3}$$

D. *Mean (MEAN):* Mean is the average gray level with respect to the central position and is given by

$$MEAN = \sum_{i=0}^{N-1} \sum_{j=0}^{N-1} ip(i,j) \tag{4.4}$$

E. *Standard Deviation (SD):* Standard deviation reflects the degree of distribution of the gray level values and the copiousness of the data in the image.

$$SD = \sqrt{\sum_{i=0}^{N-1} \sum_{j=0}^{N-1} (i * MEAN - p(i,j)^2)} \tag{4.5}$$

F. *Angular Second Moment (ANG):*

Angular second moment evaluates the consistency of textural information and is given by

$$ANG = \sum_{i=0}^{N-1} \sum_{j=0}^{N-1} p(i,j)^2 \tag{4.6}$$

G. *Correlation (COR):*

Correlation is a measure of gray tone linear dependencies in the image and hence the linear relationship between the gray levels of pixel pairs is speculated in this and is estimated as

$$COR = \sum_{i=0}^{N-1}\sum_{j=0}^{N-1}\frac{(i-\mu)(j-\mu)p(i,j)}{\sigma_i\sigma_j} \tag{4.7}$$

H. *Entropy (ENT):*

The disorderliness of an image is given by entropy. Texturally inconsistent image having very low values for many GLCM elements entails that the entropy is very large.

$$ENT = \sum_{i=0}^{N-1}\sum_{j=0}^{N-1} p(i,j)log\left(p(i,j)\right) \tag{4.8}$$

4.2 Image model

Let the image is assumed to be defined over a discrete rectangular lattice $S = (M \times N)$. Let W denotes the label process associated with the true but unknown labels and w is the realization of it. In case of color images, $w = [w^1, w^2, w^3]^T$ denote the labels associated with the three components of some color coordinate system, for instance w^1 corresponds to label associated with I_1, w^2 to label associated with I_2 and w^3 to label associated with I_3 in Ohta color space or it will correspond to the labels associated with red, green and blue components respectively in RGB color coordinate system. The label process is modeled as MRF.

Let X denotes the observed random field corresponding to the observed degraded image and is assumed the degraded version of the label process. x be the realization of it. Then we consider the following degradation model

$$X_{i,j} = W_{i,j} + Z_{i,j} \forall (i,j) \in (M \times N) \tag{4.9}$$

With lexographical ordering this is written as $X = W + Z$.

Let η denote the neighborhood system on S. By assuming the label process W

to be Markov random field (MRF) with respect to neighborhood system η, it is demonstrated by its local characteristics

$$P\left(W_{i,j} = w_{i,j} \mid W_{k,l} = w_{k,l}, k, l \in S, (k,l) \neq (i,j)\right) = P\left(W_{i,j} = w_{i,j} \mid W_{k,l} = w_{k,l}, k, l \in \eta_{i,j}\right) \tag{4.10}$$

Because W is MRF, according to Hammersly-Clifford theorem [40], through MRF-Gibb's equivalence, the joint probability distribution can be expressed as

$$P(W = w \mid \phi) = \frac{1}{Z'} e^{-U(w,\phi)} \tag{4.11}$$

The model in Eqn.(4.11)is the *a priori* distribution of the random field W. Z' is the partition function as defined in Chapter 2 . The exponential term $U(w, \phi)$ is called the energy function and takes the form $U(w, \phi) = \sum_{c \in C} V_c(w, \phi)$ and V_c which denotes the clique potential associated with clique c. The followings assumptions are made for the above mentioned degradation model in (4.9)

- $Z_{i,j}$ is statistically independent of $W_{i,j}$, for all (i, j) and (k, l) belonging to S.

- $\mathrm{w}_{i,j}$ takes any value from the set $G = (0, ..., G_m)$. Generally $G_m = 2$ for binary images and 256 for gray scaled images. In case of a color image each component is represented as a gray scale image.

4.3 MAP Estimation of Image Labels

In MRF frame work the pixel labels are estimated using the associated model parameters. Let α, β and σ are the associated model parameters in weak membrane model. Since in partially unsupervised frame work, only the number of classes are known and the model parameters are not known, model parameters are selected on ad hoc basis. Let W be the random field associated with noise free class label and w be the realization of it. W is modeled as MRF. Let X represent the observed image random field and x be the realization of the same. Let ϕ be the representation for associated model parameters. Let w^* denote the true but unknown labeling configuration and $\hat{w}$ denote the estimation for w^*. w^*

is the realization of the random field W, which is modeled as MRF. The problem is devised as pixel labeling problem and the $\hat{w}$ is found by maximum *a posteriori* probability condition,

$$\hat{w} = \arg\max_{w} P\left(W = w \mid X = x, \phi\right) \tag{4.12}$$

w is unknown and hence it can be computed using Bayes' theorem as

$$P\left(W = w \mid X = x, \phi\right) = \frac{P\left(X = x \mid W = w, \phi\right) P\left(W = w\right)}{P\left(X = x \mid \phi\right)} \tag{4.13}$$

Since X corresponds to the given image $P(X = x \mid \phi)$ is a constant quantity. $P(W = w)$ is the *a priori* probability of the labels. Therefore 4.13 can be written as

$$P\left(W = w \mid X = x, \phi\right) = P\left(X = x \mid W = w, \phi\right) P\left(W = w\right) \tag{4.14}$$

Since W is MRF, according to Hammersley-Clifford theorem, prior probability distribution in (4.13) is given as

$$P(W = w) = \frac{1}{Z} e^{-U(w,\phi)} \tag{4.15}$$

$U(w, \phi)$ is known as the prior energy and is defined as follows

$$U(w, \phi) = \sum_{c \in C} V_c(w, \phi) \tag{4.16}$$

The term $V_c(w, \phi)$ is known as clique potential and $\sum_{c \in C} V_c(w, \phi)$ is the sum of clique potentials over all possible cliques C. ϕ is the set of clique parameters and is given by $\phi = [\alpha, \beta]$. As the color image has three spectral components, V_c is written as

$$V_c(w, \phi) = \sum_{c \in C} V_c(w^{(1)}, w^{(2)}, w^{(3)}) \tag{4.17}$$

Let $\mathrm{v}_{i,j}$ represent the vertical line field and $\mathrm{h}_{i,j}$ the horizontal line field. Let $W^1_{i,j}$, $W^2_{i,j}$ and $W^3_{i,j}$ represent the class labels in each of the color components 1, 2 and 3 respectively. Then we define the following terms

$$\|W_{i,j}\|^2 = (W^1_{i,j})^2 + (W^2_{i,j})^2 + (W^3_{i,j})^2$$

$\|W_{i,j} - W_{i,j-1}\|^2 = \frac{1}{3}\sum_{q=1}^{3}\left(W_{i,j}^q - W_{i,j-1}^q\right)^2$

$f_v(W_{i,j}, W_{i,j-1}) = \frac{1}{3}\sum_{q=1}^{3}|W_{i,j}^q - W_{i,j-1}^q|$ and

$f_h(W_{i,j}, W_{i-1,j}) = \frac{1}{3}\sum_{q=1}^{3}|W_{i,j}^q - W_{i-1,j}^q|$

α and β represent external and internal field parameters of clique potential respectively. The clique potential is given by

$$V_C(w) = \sum_{i,j}\alpha\left[|w_{i,j} - w_{i,j-1}|^2(1 - v_{i,j}) + |w_{i,j} - w_{i-1,j}|^2(1 - h_{i,j})\right] + \beta\left[v_{i,j} + h_{i,j}\right] \tag{4.18}$$

The vertical line field $\mathrm{v}_{i,j} = 1$ if f_v ($\mathrm{W}_{i,j}$, $\mathrm{W}_{i,j-1}$) $\succ$ *thresh* and the horizontal line field $\mathrm{h}_{i,j} = 1$ if f_h ($\mathrm{W}_{i,j}$, $\mathrm{W}_{i-1,j}$) $\succ$ *thresh*. The value of *thresh* is found out by dividing alpha by beta.

The conditional distribution of the observed data x given the true label is often assumed to be Gaussian, and hence can be formulated as

$$P(X \mid W) = \frac{1}{\sqrt{(2\pi)^P|\Sigma|}}\exp\left(-\frac{1}{2}(x - w)^T\Sigma^{-1}(x - w)\right) \tag{4.19}$$

Where Σ is the covariance matrix and P represents the number of color components. In our work we have considered color image with three spectral components and assumed that the components are uncorrelated in Ohta color space having the same variance. Hence the Eqn. (4.19) reduces to,

$$P(X \mid W) = \frac{1}{(2\pi)^3\sigma^3}\exp\left(-\frac{1}{2\sigma^2}(x - w)^2\right) \tag{4.20}$$

From Eqns.(4.15) through(4.20) the posteriori probability in Eqn.(4.12) reduces to,

$$\hat{w} = \arg\max_w \frac{1}{Z\sqrt{(2\pi)^3\sigma^3}}\exp\left(\frac{(x - w)^2}{2\sigma^2} + U(w, \phi)\right) \tag{4.21}$$

The maximization of the above function is equal to the minimization of the following,

$$\hat{w} = \arg\min_w \left(\frac{(x - w)^2}{2\sigma^2} + U(w, \phi)\right) \tag{4.22}$$

For the color image with three spectral components Eqn.(4.22) is represented as

$$\hat{w} = \arg\min_{w} \left(\frac{\frac{1}{3}(x^{(1)} - w^{1})^2 + (x^{(2)} - w^{2})^2 + (x^{(3)} - w^{(3)})^2}{2\sigma^2} + \sum_{c \in C} V_c(w^{(1)}, w^{(2)}, w^{(3)}) \right) \tag{4.23}$$

4.4 Proposed GLCM and MRF Model Based Segmentation Approach

The proposed GLCM and MRF model based segmentation technique comprises of two stages,

i. Texture feature is extracted and optimal texture feature image is obtained in Ohta color space.

ii. Contextual feature is incorporated by modeling the feature image as described in section 4.2. MAP estimation of image labels are obtained using ICM algorithm.

In the first step, computation of GLCM and derivation of second order statistics from the GLCM is achieved. The choice of the color space also has a very significant finding, which can dramatically influence the results of the segmentation. It is found that the components of Ohta color space which are a linear combinations of red, green and blue components of the RGB color model bring about more beneficial results especially for textured and real world imagery. Hence in our approach the images are first converted from RGB to ohta color space. Then I_1, I_2 and I_3 components of the Ohta color space are utilized for obtaining texture features with the help of a moving window. In the moving window concept, each cell in the window sits over an occupied image cell. The GLCM is computed for the window taking the corresponding values of the cells of the image on which window is placed. Then the computed value is assigned to the center pixel of the window. The window is moved to next pixel and the process is repeated for the

entire image thus computing the GLCM and the required textural measures for each pixel of the image. In this way an entire image is constructed with texture values thus forming textured image of different textural features. This is represented pictorially as shown in Figure 4.4. As it is already mentioned, each cell in a window must sit over an occupied image cell and the center pixel gets the value. This condition easily reveals that the center pixel of the window cannot be an edge pixel of the image. Hence it becomes mandatory that, for a window of dimension N x N, a band of $(N-1)/2$ pixels wide around the image to stay unoccupied. This is solved by filling the edge pixels with the nearest texture calculation. For a 7×7 window, the values computed in row 4, column 4, $(R-3)$th row and $(C-3)$th column are assigned to the outer three rows and outer three columns of the image. R and C stand for the number of rows and columns of the image. As

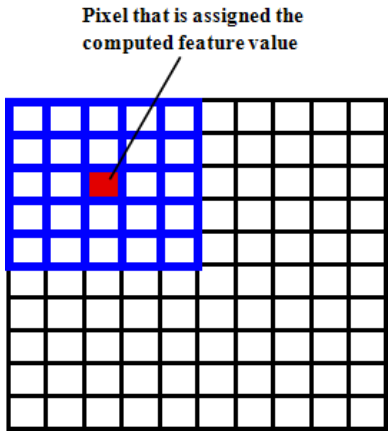

Figure 4.1: Figure demonstrating the moving window concept for the computation of GLCM and related textural features. The image is of size 10 by 10 with the window of size 5 by 5

the image edge pixels constitute a very small fraction of total image pixels, this will not lead to any major problem.The factors that influence in the computation of gray level co-occurrence matrix are (i) the number of gray levels, (ii)inter pixel distance d (iii) direction and (iv) the size of the window. The following procedure was adopted to realize the same.

1. **Selection of optimal window size and inter pixel distance:** As the success of segmentation using texture feature matrix depends largely on the

size of the window, identifying optimal window size is one of the important step in texture feature extraction.If the window size is too large, there is a chance of overlapping of two types of textures and thus bringing in fallacious spatial information. Thus, initially, in our proposed work, GLCM values were calculated for six window sizes ($3\times3, 5\times5, 7\times7, 9\times9, 11\times11 and 13\times13$). It is found that a window size of (3×3) is optimal and yields better results for the color textured images. As we have considered synthetic textured images and natural scenery images inter pixel distance of 1 is considered for computation.

2. **Selection of optimal textural feature:** The selection of optimum feature is exerted by the evaluation of texture features. The following procedure is followed, initially for a few set of images, regions of interest representing the different textures of the image are selected from the original image. Textural features as described in section 4.1 are computed for all representative texture regions. In order to realize the optimum textural feature, graphs are plotted for feature values verses each of the textures representing eight regions of interest. With respect to the discriminating capability of the feature, the optimum texture feature is selected by visually analyzing the group of texture features. This can be well understood with the help of a figure. Fig 1.2 shows the angular momentum values for different regions of interest for both the classes. It can be noticed from the figure that none of the texture matrices of I_1, I_2 and I_1 color component are able to differentiate between the classes. The values of both the classes are overlapping. Similarly the figures through 4.3(a) to 4.4(b) represent the texture matrices for contrast, correlation, dissimilarity, entropy, homogeneity and standard deviation and have overlapping class values. But it is clearly seen from the Figure 4.4(c) that texture matrix mean is able to distinguish the classes. Hence mean texture matrix is considered to be the optimal one for segmentation in our proposed work.

- **Selection of appropriate direction:** For choosing the appropriate direction, the literature suggests that any directions is appropriate, assuming the redundancy of texture in different directions. Hence GLCM has been created in a single direction 45^o. This has even helped to considerably reduce the computational time.

In the second step, segmentation of color textured image is obtained. The optimal feature image obtained in first step is assumed to be the degraded form of true labeled image. This feature image is modeled as described in Eqn. 4.9. MAP estimation of image labels are obtained using ICM algorithm as described in previous sections and the segmentation is obtained. The true label process is considered to be a Markov Random Field which incorporates contextual features along with texture and color features.

(a) Two class color textured image of size 130 × 130

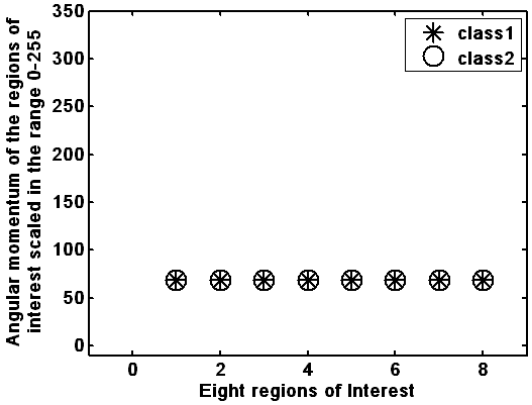

(b) Angular momentum of two classes at different locations for I_1 component

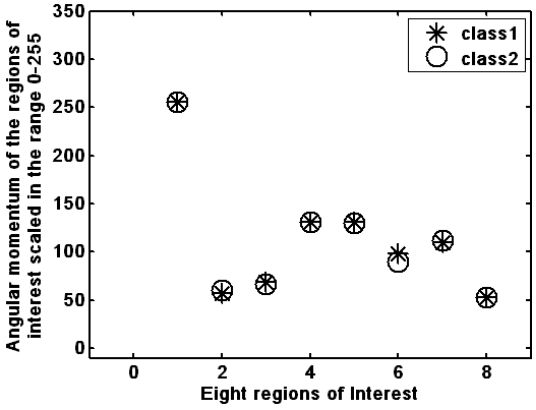

(c) Angular momentum of two classes at different locations for I_2 component

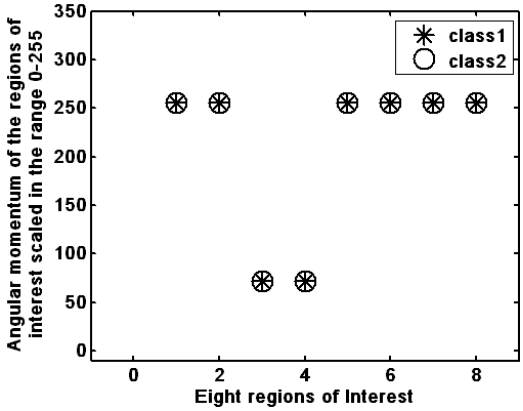

(d) Angular momentum of two classes at different locations for I_3 component

Figure 4.2: Figure showing the plot of values of angular momentum at different locations of the region 1 and region 2 of a two class image for all the three components I_1, I_2 and I_3 of Ohta color space

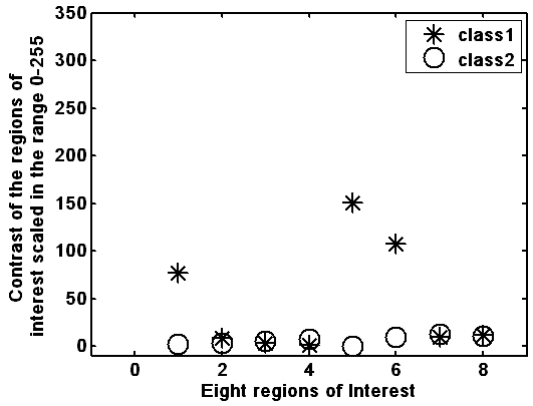

(a) Contrast of two classes at different locations

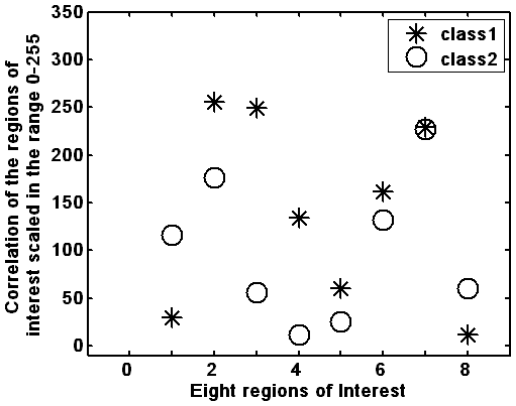

(b) Correlation of two classes at different locations

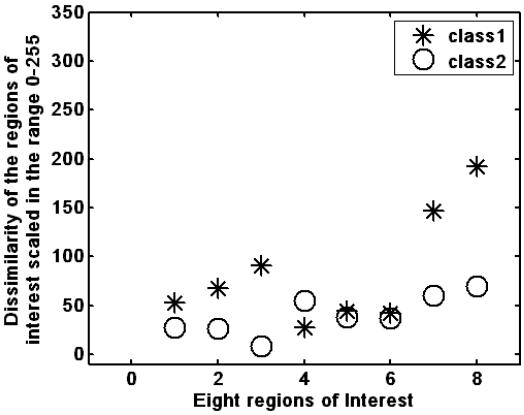

(c) Dissimilarity of two classes at different locations

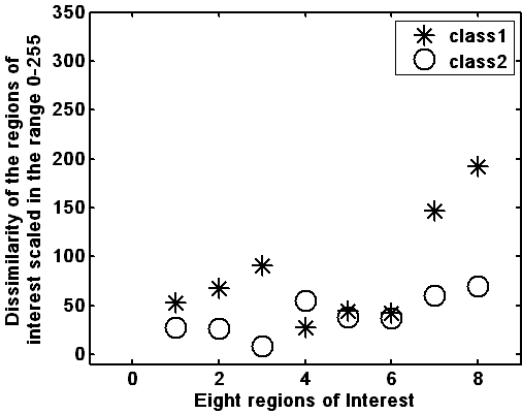

(d) Entropy of two classes at different locations

Figure 4.3: Figure showing the plot of values of contrast, correlation and dissimilarity at different locations of the region 1 and region2 of a two class image in Figure 4.2(a)

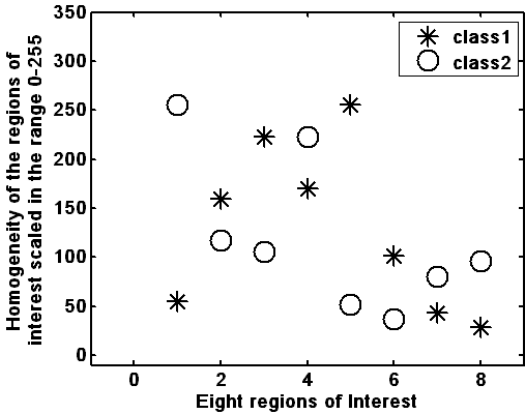

(a) Contrast of two classes at different locations

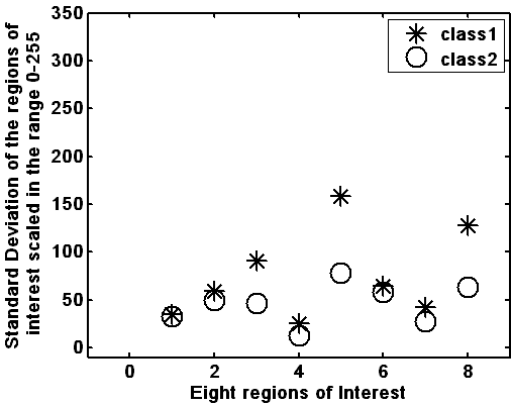

(b) Correlation of two classes at different locations

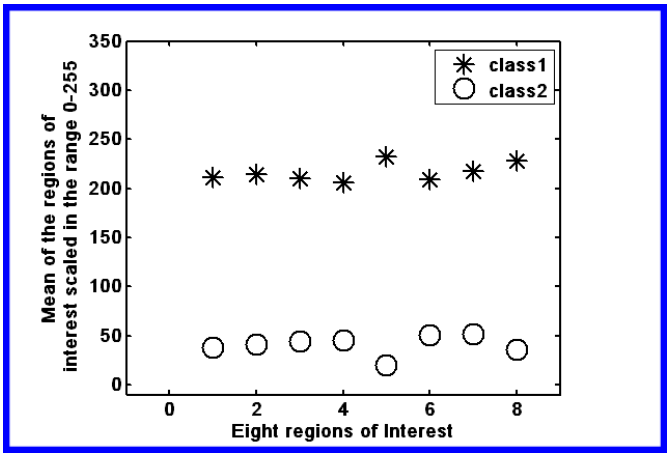

(c) Dissimilarity of two classes at different locations

Figure 4.4: Figure showing the plot of values of homogeneity, standard deviation and mean at different locations of the region 1 and region2 of a two class image in Figure 4.2(a)

4.5 Results and Discussion

In the simulation, both synthetic as well as real scenery images are considered to validate the proposed algorithm. Synthetic images consisting of 2, 3 and 4 classes are considered for simulation. Besides, few Berkely set of images are also looked at for simulation. The simulated synthetic texture images as well as real images are obtained from http://www.imageafter.com/, http://www.cgtextures.com/ and http://www.eecs.berkeley.edu/Research/Projects/CS/vision/bsds/.

Two class synthetic textured and natural scenery images:

Figure 4.6(a) shows a two class synthetic colour textured image of size (130 × 130). The image is originally a RGB image which is converted into Ohta colour space with components I_1, I_2 and I_3. As already discussed in section 4.4, mean feature matrix has been regarded as the optimal one for segmentation. However for a two class image it is noticed that mean texture matrix of I_1 and I_3 components are unable to differenciate the different classes of the image. Hence mean texture matrix of I_2 component alone is considered for segmentation of two class textured images. Figures 4.5(a), 4.5(b) and 4.5(c) show the plot of mean feature value at eight regions of interest in each of the two classes of I_1, I_2 and I_3 component respectively. After converting the image from RGB to Ohta colour space, the gray level cooccurence matrix (GLCM) and the mean feature matrix of a two class image is computed for I_2 component. The computed feature matrix is modeled as a degraded model for the MAP estimation of the true image labels. The unknown true image label process is modeled as Markov Random Field model. The model parameters of each class label (α, β, σ) are taken on *ad hoc* basis. MAP estimation of the image labels is obtained through iterated conditional modes (ICM) algorithm and the algorithm is run for 20 number of iterations for getting the optimal results. To validate that the mean feature matrix is the optimal one, all the other seven feature matrices namely angular momentum, contrast, correlation, dissimilarity, entropy, homogeneity, standard deviation obtained for I_2 component are shown for

the two class textured image in Figures 4.6(b), 4.6(c), 4.6(d), 4.6(e), 4.6(f), 4.6(g) and 4.7(d) respectively. Figures 4.7(c), 4.7(d) and 4.7(e) shows the mean feature matrices in I_1, I_2 and I_3 components respectively. It is easily identifiable from the figure that mean feature matrix of I_2 component is more suitable than I_1 and I_3 components for MAP estimation of image labels.

The first image considered is a synthetic two class textured image as shown in Figure 4.7(a). Figure 4.7(b) shows the corresponding ground truth image. The image in the RGB color space is first converted into ohta color space. GLCM texture feature matrices are computed from the image. The feature matrix in Figure 4.7(d) is modeled as degraded version of the label image and is segmented by MAP estimation using ICM algorithm. The values of model parameters α, β and σ are taken on trial and error basis. The ICM algorithm converges for the values of model parameters at $\alpha = 0.0025$, $\beta = 3.0$ and $\sigma = 5.0$. The values of the model parameters are shown in Table 4.7. Figures 4.7(f) and 4.7(h) show the segmented images using JSEG and GLCM-GMRF-ICM techniques respectively. It can visualized as well as found from Table 4.1 that the proposed method GLCM-GMRF-ICM found to be performing better than both JSEG and GMRF-GA-ICM techniques. The JSEG method has an accuracy of 96.44%, GMRF-GA-ICM has 93.69% and GLCM-GMRF-ICM has an accuracy of 98.64% which is outperforming other two methods. JSEG method has the least computation time of 15 secs, while GMRF-GA-ICM and GLCM-GMRF-ICM have 29 and 20 secs respectively.

The technique is also validated with real textured images. Figure 4.8(a) shows a real image which comprises of the regions road and grass. Figure 4.8(b) shows the corresponding ground truth image. Figsures 4.8(c), 4.8(d) and 4.8(e) shows the mean feature matrices in I_1, I_2 and I_3 components respectively. The model parameters for the MAP estimation are $\alpha = 0.0029$, $\beta = 3.06$ and $\sigma = 5.0$. The values of the model parameters are shown in Table 4.7. Figsures 4.8(f), 4.8(g) and 4.8(h) show the segmented images using JSEG, GMRF-GA-ICM and GLCM-GMRF-ICM techniques respectively. It is shown from Table 4.2 that the proposed methods GMRF-GA-ICM and GLCM-GMRF-ICM have greater accuracies than

the JSEG method. Though the computation time is less in case of JSEG technique, it does not give accurate results for real images. Overall proposed GLCM-GMRF-ICM method is more accurate than the other two methods.

Similarily, another real image of size (200×146) as shown in Figure 4.9(a) is considered for simulation. The image comprises of two regions, mud road and forest area. Figure 4.9(b) shows the corresponding ground truth image. Figures 4.9(c), 4.9(d) and 4.9(e) shows the mean feature matrices in I_1, I_2 and I_3 components respectively. Figures 4.9(f), 4.9(g) and 4.9(h) show the segmented images using JSEG, GMRF-GA-ICM and GLCM-GMRF-ICM techniques respectively.The segmented images using the proposed model uses the model parameters $\alpha = 0.0032$, $\beta = 3.42$ and $\sigma = 5.0$. Again the GLCM-GMRF-ICM algorithm outperforms the other two methods n terms of accuracy.

It can be observed from all the results of the two class images that, the proposed GLCM-GMRF-ICM technique always outperforms the other two methods. In case of synthetic textured images, sometimes the accuracy level of JSEG method becomes almost equal to that of the proposed GLCM-GMRF-ICM method. But with the real images the technique outperforms the JSEG method. This is well identified from the results of images in Figures 4.8, 4.9, 4.10 and 4.12. Especially from the results of the tree and sky image in Figure 4.12, it is clearly seen that the misclassification error of JSEG method is very high with the value 20%. Where as the proposed methods GLCM-GMRF-ICM and GMRF-GA-ICM lead this method with the percentage of misclassification error of only 1.36% and 7.31% respectively.

The techniques are tested for three class and four class images as well. For a three class image it is found that mean feature matrix of I_1 component is unable to differenciate the different classes of the image. The image can be segmented by taking the other two components I_2 and I_3 together in combination. Figure 4.13(a) shows a three class synthetic textured image. It can be observed from the I_2 and I_3 mean feature matrices as shown in Figure 4.13(d) and Figure 4.13(e) respectively that they are able differenciate only two classes when they are considered separately. But the same feature matrices when taken in combination can segment

the image accurately. Hence in our proposed approach the MAP estimation of the image labels are obtained by considering feature matrices of I_2 and I_3 components.

Figure 4.13(a) shows a three class textured image of size (180×154). Figure 4.13(b) shows the ground truth image. The MAP estimation of the image labels are obtained by taking mean feature matrices of I_2 and I_3 components and segmentation is done using ICM algorithm. Table 4.12 shows the model parameters of the image. Figures 4.13(f), 4.13(g) and 4.13(h) show the segmented images using JSEG, GMRF-GA-ICM and GLCM-GMRF-ICM techniques respectively. The performance measures are presented in Table 4.8. It is observed that JSEG method, GMRF-GA-ICM and GLCM-GMRF-ICM perform with MCE of 2.57%, 3.68% and 1.89% respectively. It is found that the proposed method GLCM-GMRF-ICM outperforms the other two methods.

Similarily all the three techniques are examined for three class real image. Figure 4.14(a) show a three class real image of size (150×300). Figure 4.14(b) shows the ground truth image. Figures 4.15(a), 4.15(b) and 4.15(c) show the segmented images using JSEG, GMRF-GA-ICM and GLCM-GMRF-ICM techniques respectively. The performance measures are presented in Table 4.9. The misclassification error is found be 5.23% for JSEG method, 3.98% for GMRF-GA-ICM method and 1.06% for GLCM-GMRF-ICM method. The model parameters are presented in Table 4.12.

Similarly the same method is followed for four class synthetic image. But in addition hue component of the HSI color space is also considered for segmentation for the sake of accuracy. Thus the image is considered to be a three band image. Figure 4.16(a) and 4.16(b) shows four class synthetic textured image and its ground truth image. The two feature matrices of I_2 and I_3 and the hue component of the HSI color space is taken for MAP estimation and segmentation of the image using ICM algorithm. Figures 4.16(f), 4.16(g) and 4.16(h) show the segmented images using JSEG, GMRF-GA-ICM and GLCM-GMRF-ICM techniques respectively. The performance measures are presented in Table 4.10. The JSEG method, GMRF-GA-ICM and GLCM-GMRF-ICM perform with MCE of 2.71%,

3.52% and 1.68% respectively. The model parameters are found in Table 4.12.

Similarly 4 class real image in Figure 4.17(a) is segmented by MAP estimation using ICM algorithm. Figure 4.16(b) shows the ground truth image. Figures 4.17(f), 4.17(g) and 4.17(h) show the segmented images using JSEG, GMRF-GA-ICM and GLCM-GMRF-ICM techniques respectively The model parameters are shown in Table 4.12. The performance measures for Figure 4.16(a) is given in Table 4.11. The misclassification error is found be 1.02%, 10.46% and 3.78% for JSEG, GLCM-GMRF-ICM and GMRF-GA-ICM methods repectively. It is found that again the proposed method outperforms the other two methods for both synthetic and real images.

4.6 Conclusion

This chapter addresses the segmentation of color textured image segmentation in Partially supervised frame work. A new scheme GLCM-GMRF-ICM is proposed which integrates the features of both gray level co-occurence matrix (GLCM) and Markov random field model (MRF). The textural features in Ohta color space are extracted using GLCM. Contextual feature is incorporated by modeling the feature image as MRF model. *maximum a posteriori* (MAP) estimation of image labels are obtained using ICM algorithm. The proposed GLCM-GMRF-ICM scheme yielded the segmentation of synthetic as well as real color textured images with better performance than the result of GMRF-GA-ICM scheme proposed in Chapter 3. The scheme works for two class, three class and four class color textured images and assumes the number of classes to be known *a priori*. Our method may be further improved for segmenting the images of more than four classes.

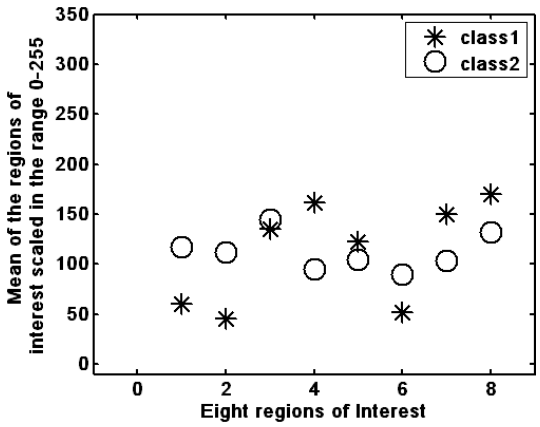

(a) Mean of two classes at different locations for I_1 component

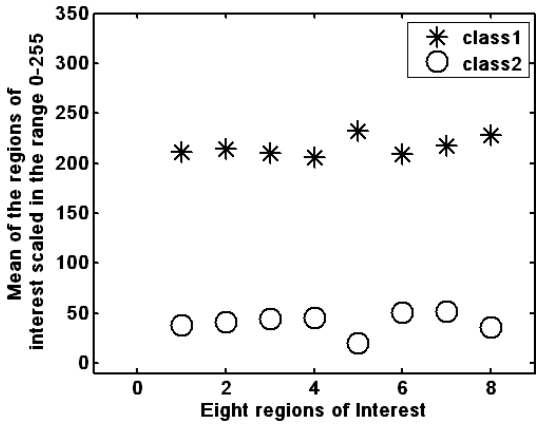

(b) Mean feature matrix of I_2 component

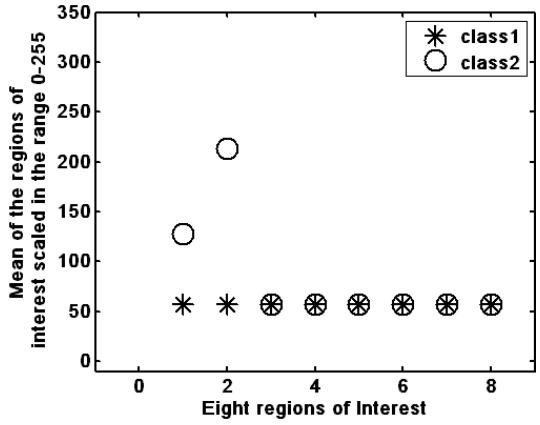

(c) Mean feature matrix of I_3 component

Figure 4.5: Figure showing the plot of values of mean at different locations of the region 1 and region 2 of a two class image in Figure 4.2(a) for all three components

(a) original Image of size 130 × 130

(b) Angular momentum feature matrix

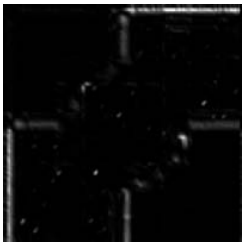

(c) Contrast feature matrix

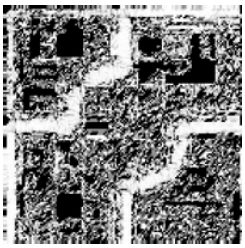

(d) Correlation feature matrix

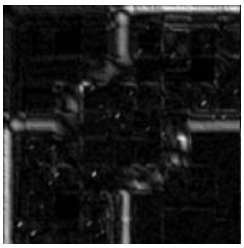

(e) Dissimilarity feature matrix

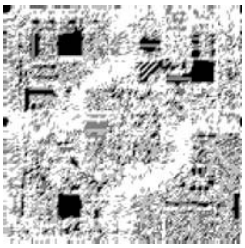

(f) Entropy feature matrix

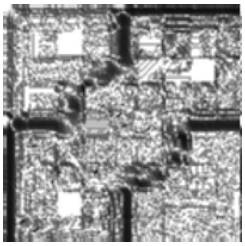

(g) Homogeneity feature matrix

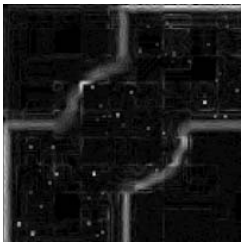

(h) Standard Deviation feature matrix

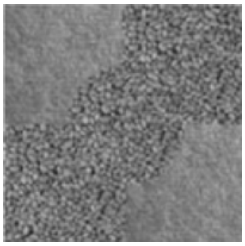

(i) Mean feature matrix of I_1 component

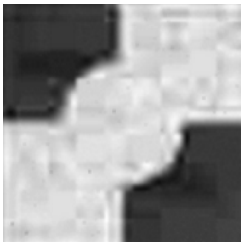

(j) Mean feature matrix of I_2 component

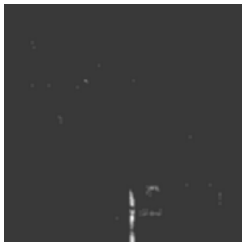

(k) Mean feature matrix of I_3 component

Figure 4.6: Figure showing the plot of values of mean at different locations of the region 1 and region 2 of a two class image in Figure 4.2(a) for all three components

(a) original Image

(b) Ground Truth

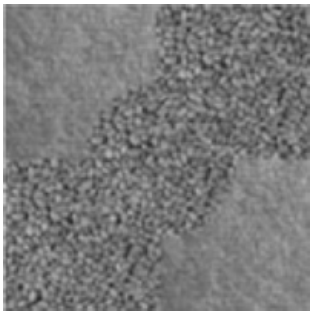

(c) Mean feature matrix of I_1 component

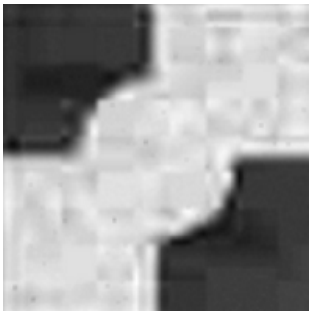

(d) Mean feature matrix of I_2 component

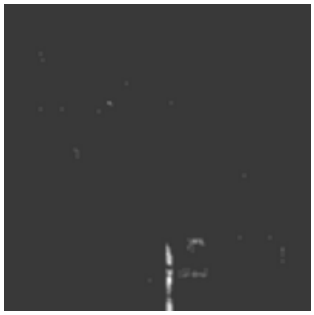

(e) Mean feature matrix of I_3 component

(f) JSEG

(g) GMRF-GA-ICM

(h) GLCM-GMRF-ICM

Figure 4.7: Segmentation of 2-class synthetic color textured image of size (130 × 130). (a)Original Image (b) Ground Truth (c) Mean feature matrix in I_1 component (d)Mean feature matrix in I_2 component (e) Mean feature matrix in I_3 component (f) Segmented image using JSEG method (g) Segmented image using proposed GLCM-MRF method

(a) original Image

(b) Ground Truth

(c) Mean feature matrix of I_1 component

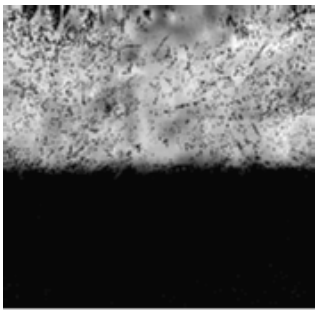

(d) Mean feature matrix of I_2 component

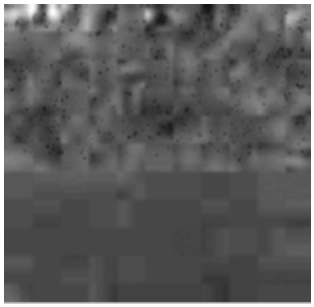

(e) Mean feature matrix of I_3 component

(f) JSEG

(g) GMRF-GA-ICM

(h) GLCM-GMRF-ICM

Figure 4.8: Segmentation of 2-class real textured image of size (175 × 170). (a)Original Image (b) Ground Truth (c) Mean feature matrix in I_1 component (d)Mean feature matrix in I_2 component (e) Mean feature matrix in I_3 component (f) Segmented image using JSEG method (g) Segmented image using proposed GLCM-MRF method

(a) original Image

(b) Ground Truth

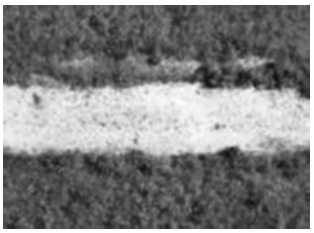

(c) Mean feature matrix of I_1 component

(d) Mean feature matrix of I_3 component

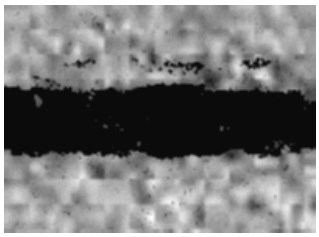

(e) Mean feature matrix of I_2 component

(f) JSEG

(g) GMRF-GA-ICM

(h) GLCM-GMRF-ICM

Figure 4.9: Segmentation of 2-class real textured image of size (200 × 146). (a)Original Image (b) Ground Truth (c) Mean feature matrix in I_1 component (d)Mean feature matrix in I_2 component (e) Mean feature matrix in I_3 component (f) Segmented image using JSEG method (g) Segmented image using proposed GLCM-MRF method

(a) original Image

(b) Ground Truth

(c) Mean feature matrix of I_1 component

(d) Mean feature matrix of I_3 component

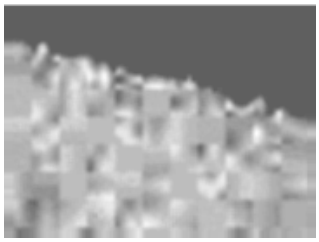

(e) Mean feature matrix of I_2 component

(f) JSEG

(g) GMRF-GA-ICM

(h) GLCM-GMRF-ICM

Figure 4.10: Segmentation of 2-class real textured image of size (180 × 135). (a)Original Image (b) Ground Truth (c) Mean feature matrix in I_1 component (d)Mean feature matrix in I_2 component (e) Mean feature matrix in I_3 component (f) Segmented image using JSEG method (g) Segmented image using proposed GLCM-MRF method

Table 4.1: Performance comparison of various segmentation techniques for Fig. 4.7

Techniques	MCE in %	Time in sec.
JSEG	3.56	15
GMRF-GA-ICM	6.31	29
GLCM-GMRF-ICM	1.36	20

Table 4.2: Performance comparison of various segmentation techniques for Fig. 4.8

Techniques	MCE in %	Time in sec.
JSEG	6.74	12
GMRF-GA-ICM	4.91	27
GLCM-GMRF-ICM	2.52	16

Table 4.3: Performance comparison of various segmentation techniques for Fig. 4.9

Techniques	MCE in %	Time in sec.
JSEG	9.09	18
GMRF-GA-ICM	3.82	32
GLCM-GMRF-ICM	2.09	20

Table 4.4: Performance comparison of various segmentation techniques for Fig. 4.10

Techniques	MCE in %	Time in sec.
JSEG	11.27	10
GMRF-GA-ICM	6.01	18
GLCM-GMRF-ICM	1.36	13

(a) original Image of size 175 × 170

(b) Ground Truth

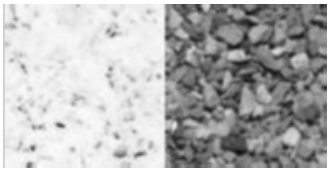

(c) Mean feature matrix of I_1 component

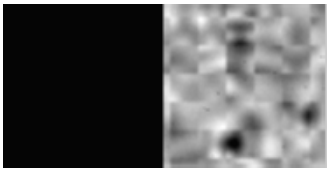

(d) Mean feature matrix of I_2 component

(e) Mean feature matrix of I_3 component

(f) JSEG

(g) GMRF-GA-ICM

(h) GLCM-GMRF-ICM

Figure 4.11: Segmentation of 2-class real color textured image of size (184 × 93). (a)Original Image (b) Ground Truth (c) Mean feature matrix in I_1 component (d)Mean feature matrix in I_2 component (e) Mean feature matrix in I_3 component (f) Segmented image using JSEG method (g) Segmented image using proposed GLCM-MRF method

(a) original Image

(b) Ground Truth

(c) Mean feature matrix of I_1 component

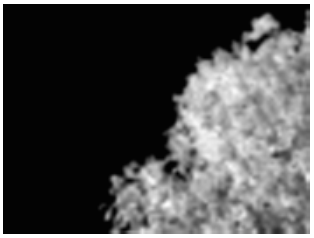

(d) Mean feature matrix of I_2 component

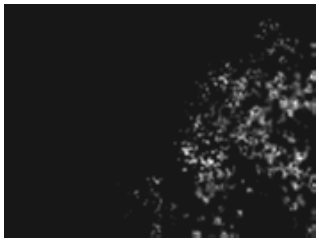

(e) Mean feature matrix of I_3 component

(f) JSEG

(g) GMRF-GA-ICM

(h) GLCM-MRF

Figure 4.12: Segmentation of 2-class real textured image of size (175 × 131). (a)Original Image (b) Ground Truth (c) Mean feature matrix in I_1 component (d)Mean feature matrix in I_2 component (e) Mean feature matrix in I_3 component (f) Segmented image using JSEG method (g) Segmented image using proposed GLCM-MRF method

Table 4.5: Performance comparison of various segmentation techniques for Fig. 4.11

Techniques	MCE in %	Time in sec.
JSEG	2.65	9
GMRF-GA-ICM	8.09	10
GLCM-GMRF-ICM	4.36	13

Table 4.6: Performance comparison of various segmentation techniques for Fig. 4.12

Techniques	MCE in %	Time in sec.
JSEG	20	9
GMRF-GA-ICM	7.31	16
GLCM-GMRF-ICM	1.36	11

Table 4.7: Model Parameters for 2 class textured images

Image	α	β	σ
Figure 4.7(a)	0.0025	3.0	5.0
Figure 4.8(a)	0.0029	3.06	5.0
Figure 4.9(a)	0.0032	3.42	5.0
Figure 4.10(a)	0.00237	3.08	5.0
Figure 4.11(a)	0.0034	4.05	5.00
Figure 4.12(a)	0.0025	3.54	5.00

(a) original Image

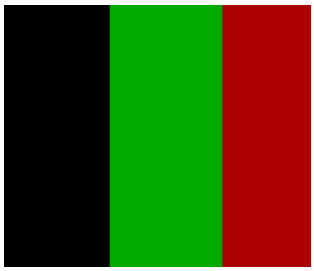

(b) Ground Truth

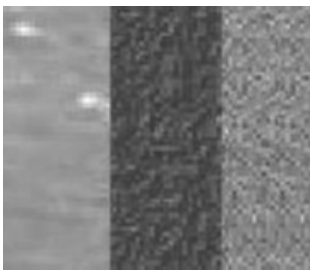

(c) Mean feature matrix of I_1 component

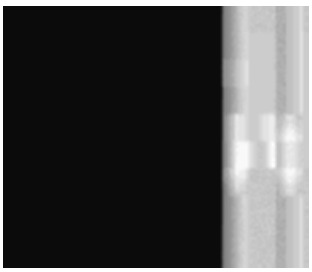

(d) Mean feature matrix of I_2 component

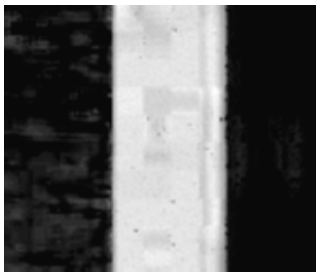

(e) Mean feature matrix of I_3 component

(f) JSEG

(g) GMRF-GA-ICM

(h) GLCM-GMRF-ICM

Figure 4.13: Segmentation of 3-class synthetic textured image of size (180 × 154). (a)Original Image (b) Ground Truth (c) Mean feature matrix in I_1 component (d)Mean feature matrix in I_2 component (e) Mean feature matrix in I_3 component (f) Segmented image using JSEG method (g) Segmented image using proposed GLCM-MRF method

(a) original Image

(b) Ground Truth

(c) Mean feature matrix of I_1 component

(d) Mean feature matrix of I_2 component

(e) Mean feature matrix of I_3 component

Figure 4.14: Segmentation of 3-class real textured image of size (150 × 300). (a)Original Image (b) Ground Truth (c) Mean feature matrix in I_1 component (d)Mean feature matrix in I_2 component (e) Mean feature matrix in I_3 component

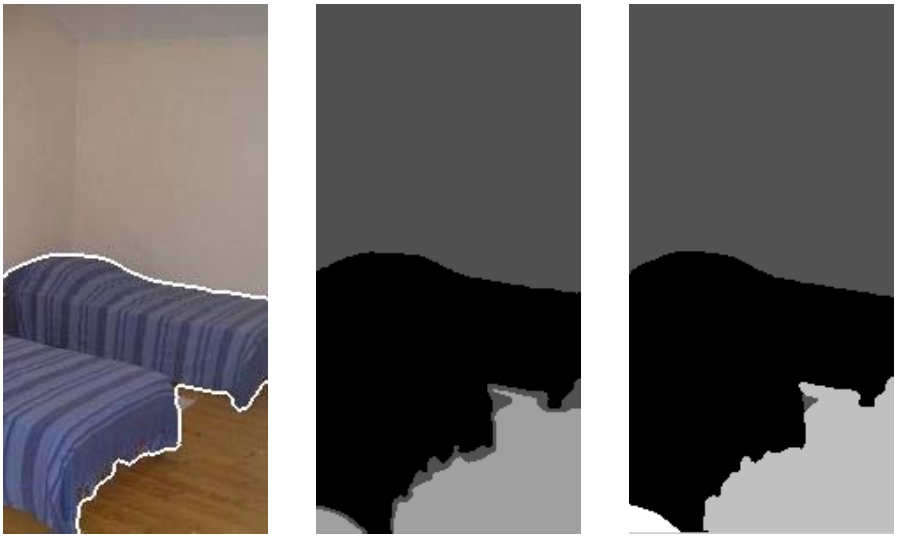

(a) JSEG (b) GMRF-GA-ICM (c) GLCM-GMRF-ICM

Figure 4.15: Segmentation of 3-class real textured image of size (150 × 300) continued from the previous page. (a)JSEG (b) GMRF-GA-ICM (c) GLCM-GMRF-ICM

Table 4.8: Performance comparison of various segmentation techniques for Figure 4.13

Techniques	MCE in ٪	Time in sec.
JSEG	2.570	12
GMRF-GA-ICM	3.68	25
GLCM-GMRF-ICM	1.89	16

Table 4.9: Performance comparison of various segmentation techniques for Fig. 4.14

Techniques	MCE in ٪	Time in sec.
JSEG	5.23	14
GMRF-GA-ICM	3.98	43
GLCM-GMRF-ICM	1.06	28

(a) original Image

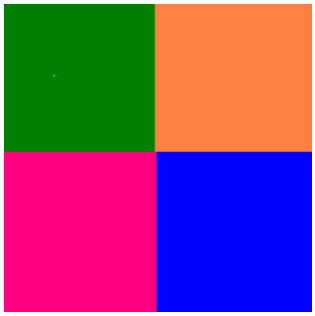

(b) Ground Truth

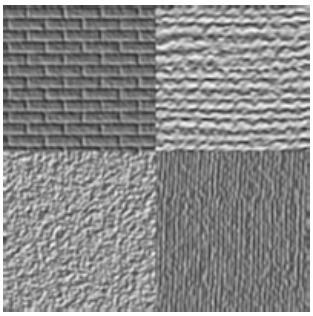

(c) Mean feature matrix of I_1 component

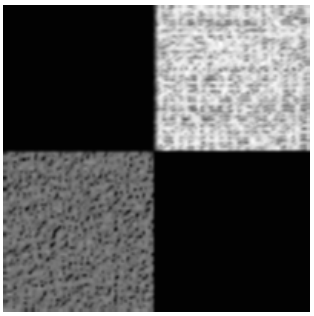

(d) Mean feature matrix of I_2 component

(e) Mean feature matrix of I_3 component

(f) JSEG

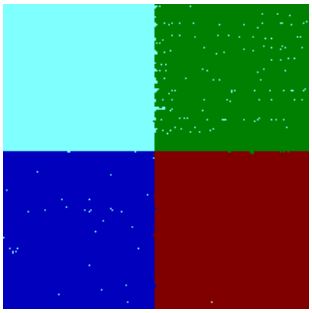

(g) GMRF-GA-ICM

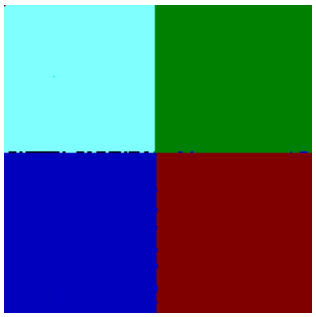

(h) GLCM-GMRF-ICM

Figure 4.16: Segmentation of 4-class synthetic textured image of size (200 × 200). (a)Original Image (b) Ground Truth (c) Mean feature matrix in I_1 component (d)Mean feature matrix in I_2 component (e) Mean feature matrix in I_3 component (f) Segmented image using JSEG method (g) Segmented image using proposed GLCM-MRF method

(a) original Image

(b) Ground Truth

(c) Mean feature matrix of I_1 component

(d) Mean feature matrix of I_2 component

(e) Mean feature matrix of I_3 component

(f) JSEG

(g) GMRF-GA-ICM

(h) GLCM-GMRF-ICM

Figure 4.17: Segmentation of 4-class real image of size (200×160). (a)Original Image (b) Ground Truth (c) Mean feature matrix in I_1 component (d)Mean feature matrix in I_2 component (e) Mean feature matrix in I_3 component (f) Segmented image using JSEG method (g) Segmented image using proposed GLCM-MRF method

Table 4.10: Performance comparison of various segmentation techniques for Figure 4.16

Techniques	MCE in ٪	Time in sec.
JSEG	2.71	15
GMRF-GA-ICM	3.52	46
GLCM-GMRF-ICM	1.68	29

Table 4.11: Performance comparison of various segmentation techniques for Figure 4.17

Techniques	MCE in ٪	Time in sec.
JSEG	1.02	7
GMRF-GA-ICM	10.46	38
GLCM-GMRF-ICM	3.78	22

Table 4.12: Model Parameters for 3 and 4 class textured images

Image	α	β	σ
Figure 4.13(a)	0.003	3.0	5.0
Figure 4.14(a)	0.00001	2.5	5.0
Figure 4.16(a)	0.0001	3.02	5.0
Figure 4.17(a)	0.0022	3.5	5.0

Chapter 5

Conclusion

The objective of this dissertation is to devise methods and strategies for the segmentation of colored textured images. This work attempts to develop partially supervised color textured image segmentation schemes that would facilitate for the automatic segmentation.

The initial portion of this thesis provides a background on Markov random field (MRF) models, gray level co-occurence metrices (GLCM) and the different color models that are used for segmentation. These are coverd in Chapter 2.

The initial part of the research work is dedicated towards devising unsupervised segmentataion of color textured images using GMRF model hybridized with Genetic algorithm (GA) which is included in Chapter 3. In this frame work the problem is cast as a pixel labeling problem and MRF model is employed to model the *a priori* unknown class labels and the observed image respectively. In this method color and contextual features are incorporated by taking iinto account the interaction within color planes and between color planes. Thus for the color image in RGB color space, each component of the RGB vector at location (i, j) will be represent as a linear combination of the color components of the neighbours and the additive noise. The GMRF model parameters are estimated by the method of maximum likelihood estimation. In the method, the probability or the likelihood of the sample data is maximized to estimate the model parameters. Image label estimates are obtained by ICM algorithm. Since ICM algorithm is sensitive to intilization condition, GA is hybridized with ICM algorithm and employed in GMRF model for better initialization and to improve the performance of segmen-

tation. By doing so, the faster convergence of ICM and global exploration of GA are achieved simultaneously. It is observed that, the proposed GMRF-GA-ICM algorithm outperformed GMRF-ICM algorithm. The algorithm yielded satisfactory results in both synthetic as well as real colour textured images. Simulated Annealing (SA) algorithm which also has the ability to converge at global optima undergoes intensive computational burden. Hence, all the three algorithm namely, SA, GMRF-ICM and GMRF-GA-ICM are compared with respect to two performance measures that is percentage of misclasification error and execution time. It is observed that, due to the incorporation of GA for initialization of ICM algorithm, misclasifiation error and computation time have been reduced in the proposed scheme.

The segmentation of color textured images based on a new notion where the textural features of GLCM are incorporated in MRF model is introduced in Chapter 4. In the proposed scheme, benefits of both GLCM and MRF model are comined together. The textural features of GLCM obtained in Ohta color space are incorporated in MRF model. It is a two stage technique where in the first stage the second order joint probabilty densities of each pixel gray level is computed using GLCM to deduce staistical measures. In this process, textural feature matrix is obtained. The Mean feature matrix which was found to be the optimal one among the feature matrices is assumed as the degraded form of the true labeled image. The unknown class labels are modeled as MRF model. The model parameters are assumed to be known *a priori* and the segmentation is obtained by MAP estimation of image labels using ICM algorithm. The number of classes are assumed to be known *a priori* and the model parametres are taken on *ad hoc* basis. The problem is formulated in partially supervised domain. The proposed scheme GLCM-GMRF-ICM is compared with the popular JSEG method proposed by Yining Deng and B.S. Manjunath and with the scheme proposed in chapter 3 with respect to two performance measures, percentage of misclassification error and computation time. The scheme outperforms the other two methods in terms of accuracy and the misclassification error has been reduced to a greater

extent. The GLCM-GMRF-ICM method is validated with different images. It is found that the technique yielded satisfactory results for both synthetic as well as real scene images. It is validated for two, three and four class images. Thus in this proposed new scheme, incorporation of contextual feature using MRF model and textural feature using GLCM in Ohta color space obtains better segmented results for colored textured images. As the proposed technique is addressed in partially supervised framework, it will be worth persuing in future a totally unsupervised approach where both the number of classes and the model parameters are unknown.

Bibliography

[1] John C. Russ. *The image processing Handbook*. CRC Press, Boca Raton, Florida, 5th edition, 2009.

[2] Milan Sonka, Vadav Hlavac, and Roger Boyle. *Image processing, Analysis and Machine Vision*. PWS publishing, California, USA, 2nd edition, 1998.

[3] Tinku Acharya and Ajoy K. Ray. *Image Processing Principles and Applications*. Wiley Interscience, New Jersy, Canada, 2005.

[4] Gilles Aubert and Pierre Kornprobst. *Mathematical Problems in Image Processing: Partial Differential Equations and the Calculus of variations*. Springer, New York, 2002.

[5] Xavier Munoz Pujol. *Image Segmentation Integrating Colour, Texture and Boundary information*. PhD thesis, Universitat de Girona, Department of Electronics, Informatics and Automation, December 2002.

[6] K.N. Plataniotis and A. N. Venetsanopoulos. *Colour Image Processing and Applications*. Springer, 2000.

[7] Stuart Geman and Donald Geman. Stochastic relaxation, gibbs distributions, and the bayesian restoration of images. *IEEE Transactions on Pattern Analysis and Machine Intelligence*, PAMI-6(6):721–741, 1984.

[8] J. Besag. On the statistical analysis of dirty pictures. *Journal of Royal Statistical Society B*, 62:259–302, 1986.

[9] Dipti Patra. *Brain MR image segmentation using Markov random field model and Tabu search strategy*. PhD thesis, National Institute of Technology, Rourkela, India, Department of Electrical Engineering, 2005.

[10] R. M. Haralick. Statistical and structural approaches to texture. In *Proceedings of IEEE*, volume 67, pages 786–804, 1979.

[11] R.M. Haralick. *Image texture survey. In Fundamentals of computer vision, edited by O. D. Faugeras*. Cambridge University Press, 1983.

[12] T. R. Reed and J. M. H. du Buff. A review of recent texture segmentation and feature extraction techniques. *CVGIP: Image Understanding*, 57(3):359–372, 1993.

[13] Chang-Tsun Li. *Unsupervised Texture Segmentation using Multiresolution Markov Random Fields*. PhD thesis, University of Warwick, Department of Computer Science, 1998.

[14] Kyong I. Chang, Kevin W. Bowyer, and Munish Sivagurunath. Evaluation of texture segmentation algorithms. In *Proceedings of IEEE Computer Society Conference on Computer Vision and Pattern Recognition*, volume 1, pages 294–299, Fort Collins, CO , USA, 23 - 25 June 1999.

[15] A.K.Jain. *The Handbook of Pattern Recognition and Computer Vision*. World Scientific Publishing Co., 2nd edition, 1998.

[16] Stephen Haddad. Texture measures for segmentation. Master's thesis, University of Cape Town, Department of Electrical Engineering, April 2007.

[17] A. K. Jain. Unsupervised texture segmentation using gabor filters. In *Proceedings of IEEE International Conference on Systems, Man and Cybernetics*, pages 14 – 19, Los Angeles, CA , USA, 4-7 Nov 1990.

[18] Mihran Tuceryan. Moment based texture segmentation. *Pattern Recognition Letters*, 15:659–668, 1994.

[19] C. Palm and T. M. Lehmann. Classification of color textures by gabor filtering. *Machine Graphics and Vision*, 11(2/3):195–219, 2002.

[20] M. Varma and A. Zisserman. Texture classification: Are filter banks necessary? In *Proceedings of the IEEE Conference on Computer Vision and Pattern Recognition, Madison, Wisconsin*, volume 2, pages 691–698, 18-20 June 2003.

[21] Morten Rufus Blas, Motilal Agrawal, Aravind Sundaresan, and Kurt Konolige. Fast color/texture segmentation for outdoor robots. In *Proceedings of IEEE/RSJ International Conference on Intelligent Robots and Systems*, Nice France, 22-26 September 2008.

[22] Sinisa Todorovic and Narendra Ahuja. Texel-based texture segmentation. In *Proceedings of IEEE International Conference on Computer Vision*, pages 1–8, Kyoto, Japan, 2009.

[23] R. M. Haralick, K. Shanmugam, and T. Dinstein. Textural features for image classification. *IEEE Transaction on Systems, Man and Cybernetics*, 3(6):610–621, 1973.

[24] P.V. Narasimha Rao, M. V. R. Sesha Sai, K. Sreenivas, M. V. Krishna Rao, B. R. M. Rao, R. S. Dwivedi, and L. Venkataratnam. Textural analysis of irs-1d panchromatic data for land cover classification. *International Journal of Remote Sensing*, 23(17):3327–3345, 2002.

[25] Anne Puissant, Jacky Hirsch, and Christiane Weber. The utility of textural analysis to improve per-pixel classification for high to very high spatial resolution imagery. *International Journal of remote Sensing*, 26(4):733–745, 2005.

[26] G. Christoulas, T. Tsagaris, and V. Anastassopoulos. Textural characterization from various representations of meris data. *International Journal of remote Sensing*, 28(3-4):675–692, February 2007.

[27] P. C. Chen and T. Pavlidis. Segmentation by texture using a co-occurrence matrix and split-and-merge algorithm. *Computer Graphics and Image Processing*, 10:172–182, 1979.

[28] R. W. Conners ans M. H. Trivedi and C. A. Harlow. Segmentation of a high resolution urban scene using texture operators. *Computer Graphics and Image Processing*, 25:273–310, 1984.

[29] C. Jacquelin, A. Aurengo, and G. Hejblum. Evolving descriptors for texture segmentation. *Pattern Recognition*, 30(7):1069–1079, 1997.

[30] Stan Z. Li. *Markov Random Field Modelling in Image Analysis*. Springer-Verlag, 2009.

[31] Dileep Kumar Panjwani and Glenn Healey. Markov random field models for unsupervised segmentation of textured color images. *IEEE Transaction on Pattern Analysis and Machine Intelligence*, 17:939–954, 1995.

[32] Santhana Krishnamachari and Rama Chellappa. Multi resolution gauss-markov random field models. *Pattern Recognition*, 30(7):1069–1079, 1997.

[33] Din-Chang Tseng and Chih-Ching Lai. A genetic algorithm for mrf-based segmentation of multi-spectral textured images. *Pattern Recognition Letters*, 20:1499–1510, 1999.

[34] Yining Deng and B.S. Manjunath. Unsupervised segmentation of color-texture regions in images and video. *IEEE Transactions on Pattern Analysis and Machine Intelligence*, 23(8):800–810, 2001.

[35] Huawu Deng and David A. Clausi. Unsupervised image segmentation using a simple mrf model with a new implementation scheme. *Pattern Recognition*, 37:2323–2335, 2004.

[36] Z. Kato and T. C. Pong. A markov random field image segmentation model for colored textured images. *Image. Vision. Comp.*, 24:1103–1114, 2006.

[37] Ralf Reulke and Artur Lippok. Markov random fields based texture segmentation for road detection. In *Proceedings of The XXI Congress of The International Society for Photogrammetry and Remote Sensing*, Beijing, 2008.

[38] Rahul Dey, P. K. Nanda, and Sucheta Panda. Constrained markov random field model for color and texture image segmentation. In *Proceedings of IEEE International Conference on Signal processing, Communications and Networking(ICSCN '08)*, pages 317–322, Chennai, India, 4-6 January 2008.

[39] Sami M. Halawani, Ibrahim A. Albidewi, M. M. Sani, and M. Z. Khan. Color image segmentation using double markov random field (dmrf) model with edge penalty function. *International Journal of Computer and Network Security (IJCNS)*, 2(5):154–159, 2010.

[40] J. Besag. Spatial interaction and the statistical analysis of the latice systems. *J.Roy. Statist.Soc.B*, 36(2):192–326, 1976.

[41] D. Geman and G. Reynolds. Constrained restoration and recovery of discontinuities. *IEEE Transactions on Pattern Analysis and Machine Intelligence*, 14(3):367–383, 1992.

[42] Sanghamitra Bandyopadhyay and Ujjwal Maulik. Nonparametric genetic clustering: Comparison of validity indices. *IEEE Transaction on Systems, Man, And Cybernetics Part C: Applications and Reviews*, 31(1):120–125, February 2001.

[43] S.N.Sivanandam and S.N.Deepa. *Introduction to Genetic Algorithms*. Springer, Berlin, Germany, 2008.

[44] Nevatia. A color edge detector and its use in scene segmentation,. *IEEE Transactions on Systems, Man and Cybernetics*, SMC-7(11):820–826, 1977.

[45] N.Funakubo. Feature extraction of color texture using neural networks for region segmentation. In *Proceedings of International Conference on Image Processing (ICIP'94)*, pages 852–856, 1994.

[46] L. Wang and D. C. He. A new statistical approach for textural analysis. *Photogrammetric Engineering and Remote Sensing*, 56:61–66, 1990.

[47] J. Wachman and R. Picard. Tools for browsing a tv situation comedy based on content specific attributes. *Multimedia Tools and Applications*, 13(3):255–284, 2001.

Publications

1. Mridula J and Dipti Patra. Unsupervised Segmentation of Multispectral Textural Images using GA-GMRF Model. *International Journal of Computer Science and Emerging Technologies*, Vol. 1, No. 4, December-2010.

2. Mridula J, Kundan Kumar and Dipti Patra. Combining GLCM features and Markov Random Field Model for Colour Textured Image Segmentation, *In Proceedings of International Conference on Devices and Communications (ICDeCom-2011)*, BIT, Mesra, India, February- 2011.

3. Mridula J and Dipti Patra. Utilization of Grey Level Co-occurrence Matrix and Markov Random Field Model for Segmentation of Colour Textured Images, *In Proceedings of International Conference on Communication, Computing and Security (ICCCS-2011)*, NIT, Rourkela, India, February-2011.

4. Mridula J and Dipti Patra. Genetic Algorithm based Segmentation of High Resolution Multispectral Images using GMRF Model, *In Proceedings of IEEE sponsored International Conference on Industrial Electronics, Control and Robotics (IECR-2010)*, NIT, Rourkela, India, December-2010.

5. Mridula J and Dipti Patra. GLCM based Colour Textured Image Segmentation using Markov Random Field Model, *In Proceedings of National Conference on Information & Communication Technology (NCICT-10)*, NYSS College of Engg. & Research, Nagpur, India, December-2010.

6. Mridula J and Dipti Patra. Gaussian Markov Random Field Model and Genetic Algorithm for color textured image segmentation, *In Proceedings of International Conference on Recent Advances in Space Technology services and Climate Change (RSTS&CC-2010)* ,Satyabhama University, Chennai, India, November-2010.